

TOPOLOGY OPTIMIZATION OF A TRIANGULAR BRACKET USING ANSYS AND EXPERIMENTAL VERIFICATION USING AN OPTICAL POLARISCOPE

*A Project report submitted in partial fulfillment of the requirements
for the award of the Degree of*

**Bachelor of Technology
in
Mechanical Engineering**

Submitted by

H. SOWMYA	319126520138
N. GANESH	320126520L24
O.V. JAYAKRISHNA	319126520154
L. GANESH	319126520148
L.Y. AJAY KUMAR	319126520150

Under the Esteemed Guidance of

Dr . RAJESH GHOSH
Associate Professor



DEPARTMENT OF MECHANICAL ENGINEERING
ANIL NEERUKONDA INSTITUTE OF TECHNOLOGY & SCIENCES
(Permanently Affiliated to Andhra University, Approved by AICTE, Accredited by NBATier-I, NAAC)
Sangivalasa, Visakhapatnam (District) Andhra Pradesh -India– 531162.

APRIL 2023

**DEPARTMENT OF MECHANICAL ENGINEERING
ANIL NEERUKONDA INSTITUTE OF TECHNOLOGY & SCIENCES
(UGC Autonomous & Permanently Affiliated to Andhra University)**

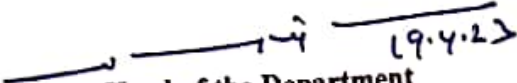


CERTIFICATE

This is to certify that the Project Report entitled "Topology Optimization of a Triangular Bracket and Experimental Verificaion using an Optical Polariscope" being submitted by O.V. Jayakrishna (319126520154), H. Sowmya (319126520138), L. Ganesh (319126520148), N. Ganesh (320126520L24), L.Y. Ajay Kumar (319126520150) to the Department of Mechanical Engineering, ANITS is a record of the bonafide work carried out by them under the esteemed guidance of Dr. Rajesh Ghosh. The results embodied in the report have not been submitted to any other University or Institute for the award of any degree or diploma.


Project Guide

Dr. RAJESH GOSH
Associate Professor
Dept. of Mechanical Engineering,
ANITS


Head of the Department

Dr. B. NAGARAJU
Professor
Dept. of Mechanical Engineering
ANITS

THIS PROJECT IS APPROVED BY THE BOARD OF EXAMINERS

INTERNAL EXAMINER

12/14/2023

EXTERNAL EXAMINER

12/14/2023

ACKNOWLEDGEMENTS

We express our deep sense of gratitude immensely to **Dr. Rajesh Ghosh**, Associate Professor, Department of Mechanical Engineering, Anil Neerukonda Institute of Technology & Sciences, Sangivalasa, Bheemunipatnam Mandal, Visakhapatnam district for his valuable guidance and encouragement at every stage of work for the successful fulfillment of students.

We are very thankful to **Prof. K. Sri Rama Krishna**, Principal, and **Prof. B. Nagaraju**, Head of the Department, Mechanical Engineering, Anil Neerukonda Institute of Technology & Sciences for their valuable suggestions.

We express our sincere thanks to the non-teaching staff of Mechanical Engineering for their kind cooperation and support in carrying on the work.

Last but not least, we like to convey our thanks to all who have contributed directly or indirectly to the completion of our work.

H. SOWMYA	(319126520138)
N. GANESH	(320126520L24)
O.V. JAYAKRISHNA	(319126520154)
L. GANESH	(319126520148)
L.Y. AJAY KUMAR	(319126520150)

ABSTRACT

Topology optimization is a mathematical approach for spatially optimizing the distribution of material within a defined region by satisfying previously established constraints and minimizing a preset cost function. In this study, the triangular bracket is redesigned using a topology optimization-based design approach using the three holes as the non-design spaces. The two left side holes are cylindrical support and a bearing load is applied to the right-hand side hole. The objective of this study is to reduce the weight of the bracket while satisfying all the design requirements related to its performance. Compare the results with the photoelasticity experiment.

Photoelasticity is an experimental technique for stress and strain analysis that is particularly useful for members having complicated geometry, complicated loading conditions, or both. The photoelastic analysis is widely used for problems in which stress or strain information is required for extended regions of the structure. It provides quantitative evidence of highly stressed areas and peak stresses at the surface and interior points of the structure. We use a dial gauge to calculate the deflection of both brackets.

Thus, observing both results we have concluded that the deflection by setting up a dial gauge, and both brackets are approximately identical. The literature survey indicates that so far, many works have been done on different topics and subjects related to topology optimization by FEA-based technique of analysis and photoelastic experiment. The discussion on the results, conclusion, and the scope of further work has also been manifested at the end of the work.

Keywords: Topology optimization, Bracket, Photoelasticity, ANSYS, Polycarbonate, FEA, Optical Polariscope, Dial Gauge, Deflection.

TABLE OF CONTENTS

Description	Page No.
ACKNOWLEDGEMENT	i
ABSTRACT	ii
TABLE OF CONTENTS	iii
LIST OF FIGURES	vi
LIST OF TABLES	vii
CHAPTER 1: INTRODUCTION	1
1.1 Topology Optimization	1
1.2 Photoelastic Experiment	1
1.3 Terminology	3
CHAPTER 2: LITERATURE REVIEW	4
2.1 Problem Statement	7
CHAPTER 3: MODELING AND ANALYSIS IN ANSYS	8
3.1 Ansys Software	8
3.1.1 Software included in Ansys	8
3.1.1.1 3D Design	8
3.1.1.2 Electronics	8
3.1.1.3 Embedded Software	8
3.1.1.4 Fluids	9
3.1.1.5 Materials	10

3.1.1.6	<i>Optical</i>	10
3.1.1.7	<i>Platform</i>	10
3.1.1.8	<i>Semiconductors</i>	10
3.1.1.9	<i>Structures</i>	10
3.1.1.10	<i>Systems</i>	10
3.2	Finite Element Analysis(FEA)	11
3.3	Mesh Definition	11
3.3.1	Meshing Methods	12
3.3.1.1	<i>Hybrid Meshing</i>	12
3.3.1.2	<i>Sweep Meshing</i>	12
3.3.2	Meshing Control	12
3.4	Analysis Process	12
3.4.1	Pre-Processing	12
3.4.2	Solving the Model	13
3.4.3	Post-Processing	13
CHAPTER 4: DESIGN CONSIDERATION AND ANSYS ANALYSIS REPORT		14
4.1	Design Procedure of a Triangular Bracket	14
4.1.1	Modal Analysis	14
4.2	Triangular Bracket Analysis Report	16
4.3	Topology Optimization Analysis	21
4.4	Design Procedure of an Optimized Bracket	23
4.4.1	Modal Analysis	23
4.5	Optimized Bracket Analysis Report	26

CHAPTER 5: PHOTOELASTIC EXPERIMENT AND ITS PROCEDURE	31
5.1 Description of Optical Polariscope	31
5.2 Experimental Procedure	32
5.3 Deflection in Dial Gauge	34
CHAPTER 6: RESULT AND COMPARISON	37
CHAPTER 7: CONCLUSION AND FUTURE SCOPE OF WORK	44
7.1 Conclusion	44
7.2 Future Scope of Work	44
REFERENCES	45

LIST OF FIGURES

Figure No.	Figure Caption	Page No.
4.1	Geometry of Triangular Bracket	14
4.2	Triangular bracket mesh	15
4.3	Triangular bracket with cylindrical support	15
4.4	Triangular Bracket with Bearing Load	16
4.5	Minimum Principal Stress in Triangular Bracket	19
4.6	Maximum Principal Stress in Triangular Bracket	19
4.7	Equivalent Stress in Triangular Bracket	20
4.8	Minimum Principal Strain in Triangular Bracket	20
4.9	Maximum Principal Strain in Triangular Bracket	20
4.10	Equivalent strain in Triangular Bracket	21
4.11	Topology Optimization on Workbench	21
4.12	Graph between Objective and Iteration Number	22
4.13	Topology Optimization of the Bracket	22
4.14	Topology Optimized Bracket	24
4.15	Triangular Bracket Mesh	25
4.16	Optimized Bracket with cylindrical support	25
4.17	Optimized Bracket with Bearing Load	25
4.18	Minimum Principal Stress in Optimized Bracket	28
4.19	Equivalent Stress in Optimized Bracket	29
4.20	Maximum Principal Strain in Optimized Bracket	29

4.21	Minimum Principal Strain in Optimized Bracket	29
4.22	Equivalent Strain in Optimized Bracket	30
5.1	Optical Polariscope	32
5.2	Photoelasticity Experiment	33
5.3	Dial gauge setup with Triangular Bracket	33
5.4	Dial gauge setup with Optimized Bracket	33
5.5	Clamps 3D Printing	34
5.6	3D Printing Clamps	35
5.7	Dial Gauge Setup for Triangular Bracket	35
5.8	Dial Gauge Setup for Optimized Bracket	35
6.1	Equivalent Stress in Triangular Bracket	38
6.2	Minimum Principal Stress in Triangular Bracket	39
6.3	Maximum Principal Stress in Triangular Bracket	39
6.4	Minimum Principal Strain in Triangular Bracket	39
6.5	Maximum Principal Strain in Triangular Bracket	39
6.6	Equivalent Strain in Triangular Bracket	39
6.7	Equivalent Stress in Optimized Bracket	41
6.8	Minimum Principal Stress in Optimized Bracket	41
6.9	Maximum Principal Stress in Optimized Bracket	41
6.10	Minimum Principal Strain in Optimized Bracket	42
6.11	Maximum Principal Strain in Optimized Bracket	42
6.12	Equivalent Strain in Optimized Bracket	42

LIST OF TABLES

Table No.	Title of the Table	Page No.
4.1	Load on the Triangular Bracket	18
4.2	Stresses in Triangular Bracket	18
4.3	Strain in Triangular Bracket	19
4.4	Topology Optimization Iteration Table	23
4.5	Load on the Optimized Bracket	27
4.6	Stresses in Optimized Bracket	27
4.7	Strain in Optimized Bracket	28
5.1	Deflection Values of Triangular Bracket	36
5.2	Deflection Values of Optimized Bracket	36
6.1	Maximum and Minimum Principal Stress in Triangular Bracket	37
6.2	Strain in Triangular Bracket	37
6.3	Maximum and Minimum Principal Stress in Optimized Bracket	40
6.4	Strain in Optimized Bracket	40

CHAPTER-1

INTRODUCTION

To increase stiffness while minimizing weight and maintaining maximum stress below a predetermined level, topology optimization is a numerical technique that is used to determine the ideal layout of structural components. To increase stiffness while minimizing weight and maintaining maximum stress below a predetermined level, topology optimization is a numerical technique that is used to determine the ideal layout of structural components. Topology optimization is a numerical technique that is used to discover the best arrangement of structural components to stiffness while minimizing weight and preserving maximum stress below a set level.

1.1 Topology optimization

The careful selection of component materials and design plays a crucial role in the development of sustainable and competitive products in various industries. To meet the high standards for strength and endurance at the component level, topology and shape optimization techniques can be employed as effective design tools in the initial stages of product design. These techniques are subfields of structural optimization, which specialize in optimizing the shape and topology of components. Thus, topology and shape optimization can be used throughout the entire process of component development to construct a robust and efficient component design.

1.2 Photoelastic Experiment

Photoelasticity is an experimental technique used to analyze the stress and strain of members with complicated geometry or loading conditions. Unlike analytical methods which involve mathematical solutions that can be time-consuming and cumbersome, photoelasticity is a suitable analytical technique for such cases. This experimental technique is based on the property of transparent, crystalline solids that produce fringes when a load is applied to the model and observed through polarized light. By analyzing these fringes, the stress and strain distribution in the material can be determined. This method is commonly used in academic research to study complex structures and materials. It requires a formal approach as it involves technical terminology and analysis that requires

precision and accuracy.

This effect is the result of the refraction of the concentrated light by the diffraction of light due to the internal distortion of the model due to the operation of external cargo. The circumferences give all stress distribution and allow the dimension of their direction and magnitude at any point within the model. The circumferences are attained due to the property of material called birefringence, since the refractive indicator of material changes by the operation of external cargo on the material. An optic system is needed for the trial in photoelasticity called polariscope. A polariscope consists of colorful rudiments given as a light source, polarizer, quarter-wave plates, and analyzer. The birefringent property of the material leads to the conformation of borderline patterns that depend on the external cargo applied to the instance. The borderline attained is observed, captured with a high-resolution CCD camera, and saved in a computer. The borderline patterns are anatomized to gain information about the stress of the instance. Borderline patterns attained in the polariscope correspond to broad borderline bands with different extents and different colors of borderline depending upon the source of light being used. The photoelastic fashion is used to study a prototype made of transparent material, having analogous parcels to that of a model. The prototype model is subordinated to analogous loading conditions like the factual workload conditions, which take to a distortion. The polariscope used in photoelasticity allows the establishment of the light propagation airplane and thus, the difference between the two factors of main stress as well as the direction of main stress.

1.3 Terminology

Polarizer: A filter for converting randomly polarized light into plane polarized light; which is located immediately in front of the light source.

Analyzer: A Filter at the viewing end of the polariscope. The polarizer and analyzer are optically identical and are thus named to distinguish their respective functions.

Quarter Wave Plates: An optical element for inducing $\frac{1}{4}$ of a wavelength of relative retardation between two spatially perpendicular component light rays. The transmission polarizer contains two-quarter wave plates – one in conjunction with the polarizer, and

one with the analyzer.

Plane Polarized Light: Light characterized by having transverse vibrations limited to a single plane for a ray; or to parallel planes for a beam.

Circularly Polarized Light: Light in which the plane of polarization rotates continuously with the propagation of the light ray. Circular polarization is produced when the vibration of the two-component ray of equal amplitude is perpendicular to each other in space and $1/4$ of a wavelength out of phase.

Fringe: Generically, colored or black lines, bands, or areas forming the photoelastic pattern, representing loci of constant difference in principal stresses. Specifically, in the case of isochromatic fringes, the tint-of-passage in white light, or the centers of the dark bands in monochromatic light.

Fringe Order (N): Ordinal numerical designation assigned to an isochromatic fringe. N equals the magnitude of the birefringence at a point (expressed in fringes), and is proportional to the difference in principal stresses at that point.

Isochromatic: A fringe (single-colored in white light, essentially black in monochromatic light) representing a locus of constant difference in principal stresses ($S_x - S_y$) as the locus of constant maximum stress.

Isoclinic: A black line representing a locus of constant directions of principal stresses, or in other words, constant inclinations of the principal axes to an arbitrary reference axis.

Monochromatic Light: Light of only one wavelength.

Principal Stresses: The algebraically maximum and minimum normal stresses at a point. The principal stresses coincide in direction with the principal strains in isotropic materials having the same elastic properties in all directions.

CHAPTER-2

LITERATURE REVIEW

Before going with the project, a brief study on papers related to the **Topology Optimization of a Triangular Bracket using ANSYS and Experimental Verification using an Optical Polariscope** was done. Many authors portrayed different ideas related to their works on Topology Optimization and Photoelastic Experiments. The different papers reviewed are listed below

Hirmukhe et.al. [1] introduced a method for the automatic analysis of photoelastic fringe patterns. The examination of color-type photoelastic fringes is the study's main objective. The difference between a sample's primary stresses is quantitatively evaluated by automatically recording and analyzing color fringes. Color photoelasticity, one of many methods described in the literature, is picked as the strategy's foundation because it requires the least amount of operator involvement. This study proposes a calibration based on average and harmonic filtering, two distinct filtering techniques. The suggested technique is assessed using an experimental set-up of a polariscope, a load system, and a CCD-type camera. For both calibration filtering techniques, experimental data are compared to the analytical solution of a disc under discrete compression.

Pathak et.al. [2] studied changes in the stress fields surrounding openings in response to the simulated breakdown of opening support and increases in room dimensions using a two-dimensional transparent photoelastic model of several underground chambers. To more precisely characterize the locations of fringe lines on the photos and to analyze the variation of stress fields under various engineering excavations, photographs of the photoelastic fringes were scanned using an Eikonixscan camera and then processed by a computer. The gradient process was thought to be a useful method for determining photoelastic stress in the study since it increased the local radiometric variability of the fringe lines. For a comparison of the boundary stresses under various engineering circumstances, the approach also gave information on fractional fringe orders.

Felippa et. al. [3] has performed a photoelasticity experiment, and their findings suggest that two quarter-wave plates were employed to remove the isoclinic fringes since the

isochromatic fringe pattern was created with circularly polarized light. The values of the major stress differential in the model along the vertical axis of symmetry, particularly in the vicinity of the contact zone, are obtained using the isochromatic fringes. The fringe orders can only be reliably determined by taking a close-up of the contact zone. The initial isochromatic's fringe order, which was employed by the author, is $N=0.5$ and starts at the bottom. In contrast, in the bottom section of the model, where the load is dispersed over the entire region of contact of the model with the loading frame, stresses were significantly lower and reached a maximum value of $N=32.5$ as they moved closer to the zone of highest shear stress.

Haciane et. al. [4] presented a study on an epoxy circular disc's elastic stress analysis. The elastic stress distribution on the disc's face has been calculated using the elasticity theory as a method. Two specimens made of photoelastic materials are created in order to validate the stress distribution predicted analytically, and they are then tested on a refractive polariscope. The two samples are spherical discs. By putting the disc in a polariscope diametrically, stress on the disc is identified. The pattern, color, and counting of fringes that form when discs are stretched in the presence of monochromatic polariscope lights form the basis of the experimental stress analysis. To validate the numerical method that we suggested in this paper, the stress distribution expressions are implemented in MATLAB, and these characteristics are contrasted with the experimental characteristics overall.

Etsion et. al. [5] demonstrated that transparent, polycarbonate medical parts may be evaluated for molded-in or applied loads quickly and without causing damage using photoelastic testing. Samples can be seen through straightforward, low-cost polarizing filters to reveal details on the direction and intensity of pressures. The test method can be applied as a quality check at the molding press if the variation in fringe patterns can be linked to a variation in a crucial part performance parameter.

Hughes et. al. [6] described in the study can be used to measure internal stresses in arbitrary constructions with complex geometry and complex loadings. Comparing the photoelastic technique to time-consuming analytical solutions and mathematical equations, it is far simpler and less demanding for situations involving models with arbitrary shapes. This method gives accurate full-field estimates of the difference between the main normal

stresses in the model's plane. Both static and dynamic inquiry can be made using this strategy. The value of non-vanishing principal normal stress throughout the model's perimeter, where the stresses are often higher, is only provided by photoelasticity. The image of the fringe pattern can be captured and processed much more quickly and easily with the aid of digital photoelasticity. The methodology is dependable and deserving of adoption for analysis, as demonstrated by the closed-form solution that is produced by photoelasticity and other analytical techniques.

Loqman et. al. [7] describe creating density-based topology optimization techniques for several difficult dynamic structural issues. To achieve optimum material distributions for the structures, we first present a normalization technique for elastodynamics that decreases frequency response and enhances the numerical stability of the bi-directional evolutionary structural optimization (BESO). Next, a hybrid interval uncertainty model is used to characterize uncertainties effectively in dynamic structural optimization to account for uncertainties in real-world engineering issues. A robust, uncertainty-insensitive dynamic topology optimization that drastically cuts down on computing costs is implemented using a perturbation method. We also incorporate an interval field uncertainty model into the dynamic topology optimization. The method is used for topology optimization in single-material, composite, and multi-scale structures.

Baek et. al. [8] focuses on the feature-driven approach to optimizing shape and topology. By combining the level-set functions for shape optimization with the weighted B-spline FCM, a quick and adaptable design method is offered. The approach is broadened to include issues where the Dirichlet boundary and free bounds are simultaneously optimal structural supports. By using parametric boundary representation and structural analysis with fixed mesh, the parametric and implicit methods for form optimization are combined. Engineering features are viewed as fundamental design primitives in the feature-driven topology optimization method, which aims to achieve topology variation by optimizing the arrangement and shape of relevant features.

Bhimaraju et. al. [9] the study includes current techniques for computational topology optimization and discusses any methods of refinement used to produce a solution that can be manufactured, with a special emphasis on techniques employed in automobile sheet metal forming. The amount of manual user input required to produce a Computer-Aided

Design (CAD) model representation of the producible solution is examined with these methodologies.

Patil et. al. [10] delivered a report on the use of SolidWorks and solidThinking Inspire to optimize the topology of a mounting bracket. When you want to make a design better or create a new part that must fit in a given area, be light, and endure a certain amount of force, topology optimization might be employed. It works by shaping a block of material by removing material, decreasing or maximizing part mass, displacement, or compliance to meet predetermined constraints like maximum stiffness or permitted amount of deformation. Numerous sectors have benefited from topology optimization's decreased weight connected to cost benefits.

Frankovský et. al. [11] have given the reference, and brackets that are topologically optimized are made using the EBM technique before being put through the hot isostatic pressing (HIP) process. With the aid of topology optimization based on finite element analyses (FEA), the weight of the engine bracket is decreased by 32%. The impact of various loading scenarios is also examined on the topologically enhanced and EBM-built Inconel 718 bracket. Using a specially designed fixture, the reference and topologically optimized brackets are put through tensile testing. The area under the "Load vs. Tensile Extension" curves is then computed to derive average energy values using software, and a 16.3% gain in energy is seen.

Karalekas et. al. [12] has released a paper that topologically optimizes four different bracket styles for loading circumstances. A rectangular building served as the first design space. The form came together to form a truss-like framework. At the concept stage of design, topology optimization is applied. Finding the ideal material distribution or arrangement at the concept stage can be very challenging for the designer. The area of the truss members can be used as a design variable to further optimize the weight of this truss-like construction. under various limitations, such as members' stress and deformation. By solely taking into account the elements with pseudo-densities between 0.223 and 1, the ideal shape has been found.

Lalitha et. al. [13] has given the reference, and brackets that are topologically optimized are made using the EBM method before being put through the hot isostatic pressing (HIP)

process. With the aid of topology optimization based on finite element analyses (FEA), the weight of the engine bracket is decreased by 32%. The impact of various loading scenarios is also examined on the topologically enhanced and EBM-built Inconel 718 bracket. Using a specially designed fixture, the reference and topologically optimized brackets are put through tensile testing. The area under the "Load vs. Tensile Extension curves are then computed to derive average energy values using software, and a 16.3% gain in energy is seen.

2.1 Problem Statement:

In the literature, several researchers have conducted Topology Optimization on a variety of structures. The researchers have analyzed different load and boundary conditions, and have implemented Topology Optimization on various materials. By conducting these analyses, these researchers have been able to understand the behavior and performance of different types of structures under different conditions. The authors perform the Photoelastic Experiment using Optical Polariscopes apparatus. By Photoelastic Experiment, the researchers study the fringes in the photoelastic material. They also calculated the stress induced in the photoelastic model by Photoelastic Experiment.

CHAPTER-3

MODELING AND ANALYSIS IN ANSYS

The purpose of this chapter is to provide an overview of the Ansys software and modeling and analysis in Ansys.

3.1 Ansys Software

Analyzing software called ANSYS is utilized in both civil and mechanical product design. It solves issues with numerical methods that are computer-based. ANSYS Inc. developed the FEA software. It is frequently employed in the sector to analyze solutions. It can solve a huge variety of issues. Large, highly nonlinear, complicated, and engineering-driven models are beneficial. In order to analyze strength, elasticity, and temperature, it is used to stimulate computer simulations of structures, electronics, or machine components. It makes extensive use of the ANSYS workbench system for simulation.

3.1.1 Software included in Ansys

3.1.1.1 3D Design

Use the 3D design software Ansys Discovery to explore concepts, iterate, and invent quickly. You may design and optimize items that are lighter and smarter using simple tools.

3.1.1.2 Electronics

Ansys software can uniquely simulate electromagnetic performance across component, circuit, and system design, and can evaluate temperature, vibration, and other critical mechanical effects.

3.1.1.3 Embedded Software

Ansys provides a model-based embedded software development and simulation environment with a built-in automatic code generator to accelerate embedded software development projects.

3.1.1.4 Fluids

Ansys CFD goes beyond qualitative results to deliver accurate quantitative predictions of fluid interactions and trade-offs.

3.1.1.5 Materials

Ansys software ensures accurate, consistent, traceable materials information every time and provides the tools you need to support design, research, and teaching.

3.1.1.6 Optical

Ansys optical simulation software uniquely simulates a system's optical performance and evaluates the final illumination effect.

3.1.1.7 Platform

The Ansys simulation platform delivers the broadest suite of best-in-class simulation technology and unifies it with your custom applications, CAD software and enterprise business process tools such as PLM.

3.1.1.8 Semiconductors

Ansys empowers customers with multi-physics simulations to simultaneously solve power, thermal, variability, timing, electromagnetics, and reliability challenges across the spectrum of chip, package, and system to promote first-time silicon and system success.

3.1.1.9 Structures

With the finite element analysis (FEA) solvers available in the suite, you can customize and automate solutions for your structural mechanic's problems and parameterize them to analyze multiple design scenarios.

3.1.1.10 Systems

As product complexity grows so does the challenge of integrating individual components within a system to ensure they work together as expected.

3.2 Finite Element Analysis(FEA)

There are three broad methods to solve complex engineering problems: analytical methods, experimental methods, and numerical methods. While analytical methods provide accurate solutions, they are limited to minimal geometries. Experimental methods can give accurate results, but they are costly, and in most cases not feasible financially. Finite element analysis (FEA), a numerical method to solve engineering problems, is a very versatile and comprehensive numerical technique that provides reliable engineering solutions. The most salient feature of FEA is the discretization of a given domain into a set of simple sub-domains called finite elements. The more the number of these finite elements, the more accurate the modeling and the subsequent analysis. The finite element method is a mathematical procedure based on solving differential equations as best as possible. A differential equation is any equation that contains derivatives, either ordinary or partial. They can be ordinary, partial, or linear. From an engineering perspective, differential equations are important because they represent the language in which physical laws are expressed. FEA aims to transform the differential equations of a system into a set of linear equations, which can then be solved by computer software.

3.3 Mesh Definition

The mathematical representation of a physical system that includes a part or assembly, material properties, and boundary conditions is called finite element analysis (FEA). In a number of circumstances, product behavior in the actual world cannot be closely reproduced by computations performed by hand. By precisely describing physical processes using partial differential equations, a general methodology like FEA offers an easy way to express complicated behaviors. Design engineers and specialists can use FEA now that it has developed and become more accessible.

One of the most crucial processes in carrying out an accurate simulation using FEA is meshing. A mesh is composed of elements that have nodes, or coordinate locations in space that can vary depending on the element type and which describe the geometry's shape. Uneven forms are difficult for an FEA solver to work with, but typical shapes like cubes make it much happier. Meshing is the process of transforming amorphous shapes

into "elements," which are more discernible volumes.

3.3.1 Meshing Methods

3.3.1.1 Hybrid Meshing

By combining hex and text elements, the Multizone method in Mechanical enables you to mesh various portions of the geometry using various techniques. As a result, you can create more local control meshes and perform less geometry preparation.

3.3.1.2 Sweep Meshing

When using sweep meshing, the mesh "sweeps" through the volume and faces to produce a useful mesh with standard dimensions. The sort of analysis (explicit or implicit) or physics you are solving for, as well as the amount of precision you want to attain, usually determine the mesh method to utilize. Cartesian meshing and layered tests are two further approaches that are utilized for certain studies, such as additive manufacturing.

3.3.2 Meshing Controls

Mesh controls allow for a more accurate mesh. Instead of a global mesh that meshes the entire CAD with the same technique, Ansys Mechanical gives you the ability to manipulate local meshes. Local scaling, refinement, and sphere of influence defeaturing of the geometry are a few examples of local meshing controls.

3.4 Analysis Process

3.4.1 Pre-Processing

Users can create geometry, define materials, and produce element mesh using the Ansys preprocessor. Users can solve difficulties using the Ansys processor.

- Define the type of Analysis

ANSYS provides a wide variety of analyses for real-life problems for mechanical and other engineering problems. Static Structural analysis is used for solving current problems.

- Define Engineering Data for Analysis

The material that is considered for the bracket is polycarbonate. The properties are given in engineering data.

- Define Boundary Conditions for Analysis Left-side holes are cylindrical support and a bearing load is applied to the right-hand side hole.

3.4.2 Solving the Model

The model nodes, elements, restraints, and loads, the analysis part of the model is ready to begin. The system can determine approximately the values of equivalent stress and principal stresses.

Analysis requires the following information:

- Nodal point
- Element connecting the nodal points
- Material and its physical properties
- Boundary conditions, which consist of loads and constraints

Analysis options: how the problem will be evaluated.

3.4.3 Post-Processing

The post-processing task generates the equivalent stresses and principal stresses induced in the bracket.

The Ansys post-processor allows visualization and listing of results in a tabular form or as printouts.

CHAPTER-4

DESIGN CONSIDERATION AND ANSYS ANALYSIS REPORT

We provide a summary of the design considerations we take into account when designing the bracket and Ansys analysis report on both the original bracket and the optimized bracket in this chapter.

4.1 Design Procedure of a Bracket in Ansys

4.1.1 Modal Analysis

Engineering Data: Verify the engineering information to make sure the right material is chosen (in our case it will be Polycarbonate).

Geometry: Open up SpaceClaim to create our geometry. We will click on the origin to begin the line and then enter 90 millimeters vertically upwards. Draw a line horizontally and enter 60 millimeters and finish off by joining the two points. We use a pulling tool to create corners of a 6mm radius. At the snap points, we draw a 6 millimeters circle. Extrude the bracket by 5 millimeters. The bracket geometry is shown in Figure 4.1.

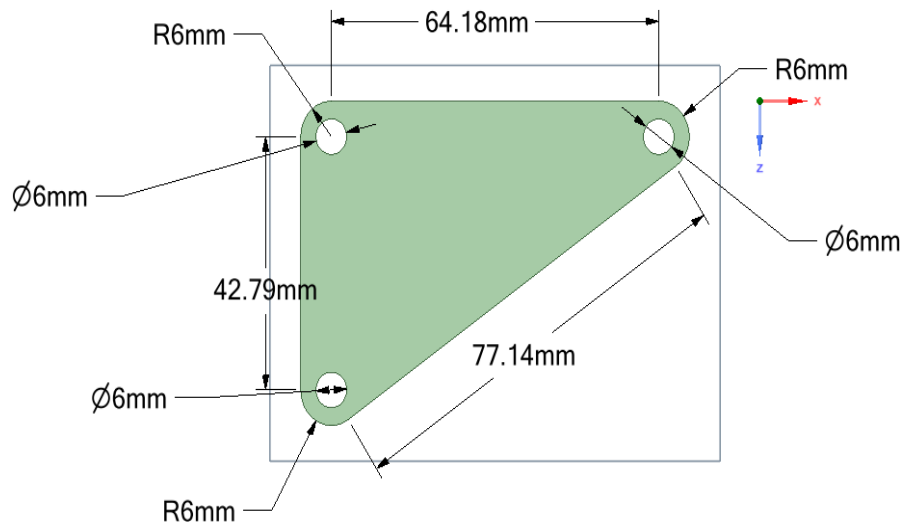


Figure 4.1: Geometry of Triangular Bracket

Mesh: Having established our loads and boundary conditions, we leave SpaceClaim and enter Mechanical. To more accurately capture the round corner details, create a mesh using the "Proximity and Curvature" size. The triangular bracket meshing is shown in Figure 4.2.

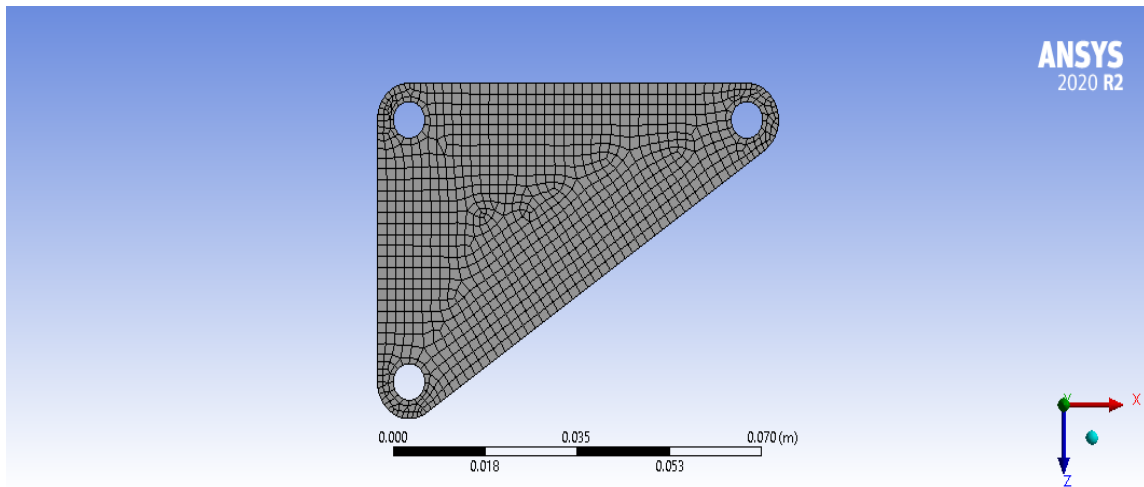


Figure 4.2: Triangular Bracket Mesh

Support and Force Component:

Make the tangential component free and add two cylindrical supports. 30N of the additional bearing load was added in the Z direction. Figures 4.3 and 4.4 depict the triangular bracket with cylindrical load and bearing load in Ansys.

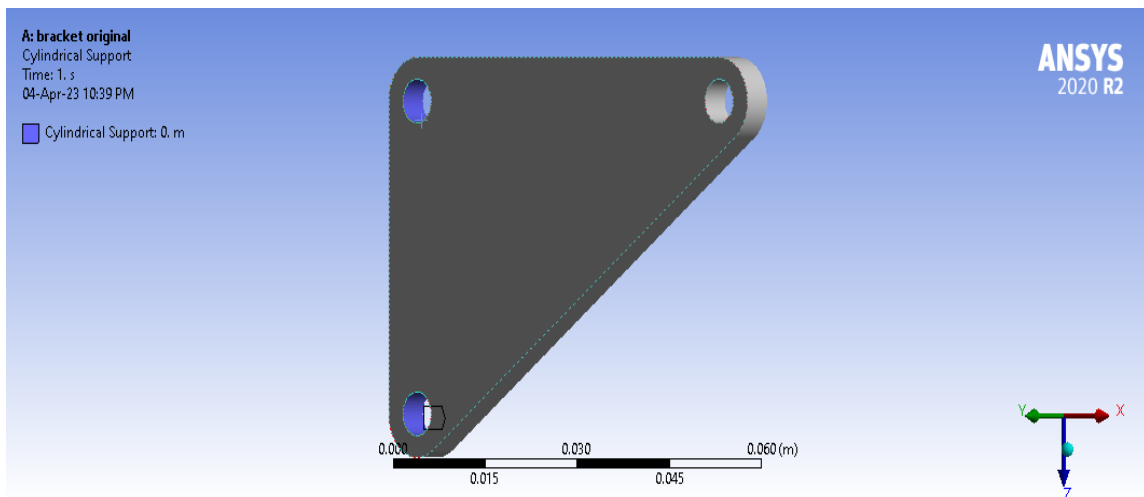


Figure 4.3: Triangular Bracket with Cylindrical Support

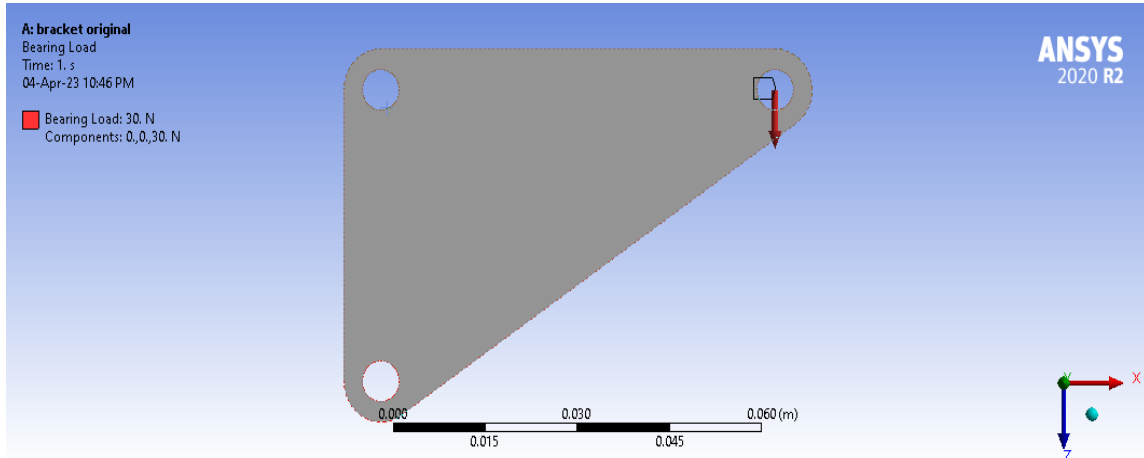


Figure 4.4: Triangular Bracket with Bearing Load

Add Equivalent Stress results, Maximum and Minimum Principal stress, and Equivalent Strain results, Maximum and Minimum Principal strain of the bracket in the bracket. Solve to view the stress and strain results.

4.3 Triangular Bracket Analysis Report

Material Data	polycarbonate
Unit System Metric	(m, kg, N, s, V, A) Degrees rad/s Celsius
Angle	Degrees
Temperature	Celsius
Length X	7.6183 cm
Length Y	0.5 cm
Length Z	5.4789 cm
Volume	12.531 cm ³
Mass	98.365 g
Nodes	24277

Elements	4935
Centroid X	-6.0967 cm
Centroid Y	0.25 cm
Centroid Z	2.0139 cm
Moment of Inertia Ip1	122.12 g•cm ²
Moment of Inertia Ip2	536.49 g•cm ²
Moment of Inertia Ip3	418.47 g•cm ²
Growth Rate	(1.85)
Max Size	(0.93972 cm)
Mesh Defeaturing	Yes
Defeature Size	Default (2.3493e-003 cm)
Capture Curvature	Yes
Curvature Min Size	Default (4.6986e-003 cm)
Curvature Normal Angle	Default (70.395°)
Capture Proximity	Yes
Proximity Min Size	Default (4.6986e-003 cm)
Num Cells Across Gap	Default (3)
Proximity Size Function	
Sources	Faces and Edges
Bounding Box Diagonal	9.3972 cm
Average Surface Area	5.8211 cm ²

Table 4.1 displays the Triangular Bracket's load conditions. Tables 4.2 and 4.3 in Ansys display the Equivalent Stress and Strain results as well as the Maximum and Minimum Principal Stress and Strain data.

Table 4.1: Load of the Triangular Bracket

Object Name	Bearing Load	Cylindrical Support
Geometry	1 Face	2 Face
X Component	0 N	
Y Component	0 N	
Z Component	30 N	
Suppressed	No	No
Radial		Fixed
Axial		Fixed
Tangential		Free

Table 4.2: Stresses in the Triangular bracket

Object Name	Equivalent Stress	Minimum Principal Stress	Maximum Principal Stress
Minimum	5465.2 Pa	-2.1883e+006 Pa	4.5562e+005 Pa
Maximum	2.9969e+006 Pa	3.5752e+005 Pa	2.7801e+006 Pa
Average	5.2335e+005 Pa	-3.1166e+005 Pa	2.3117e+005 Pa

Table 4.3: Strain in the Triangular bracket

Object Name	Equivalent Strain	Minimum Principal Strain	Maximum Principal Strain
Minimum	5.051e-08	-9.1644e-06	1.0218e-08
Maximum	1.5e-05	-1.915e-08	1.28e-05
Average	2.638e-06	-1.906e-06	1.622e-06

Figures 4.5, 4.6, and 4.7 display the Maximum, Minimum, and Equivalent Stresses from the Ansys Analysis. Figures 4.8, 4.9, and 4.10 display the Maximum, Minimum, and Equivalent Strain from the Ansys Analysis.

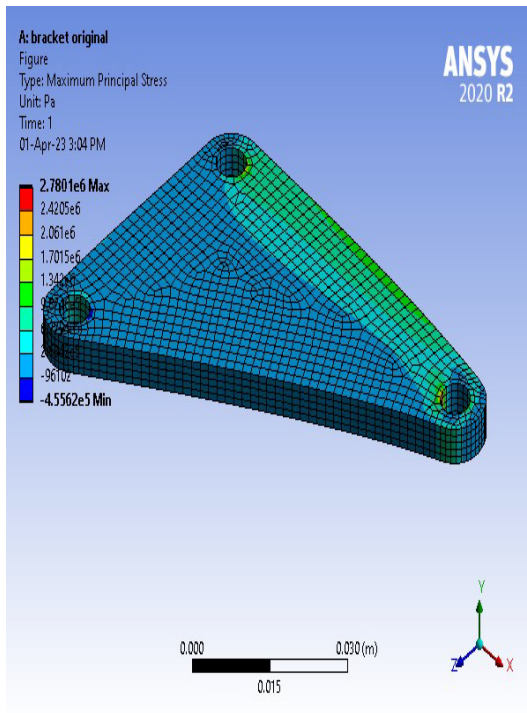


Figure 4.5: Maximum Principal Stress in original Bracket

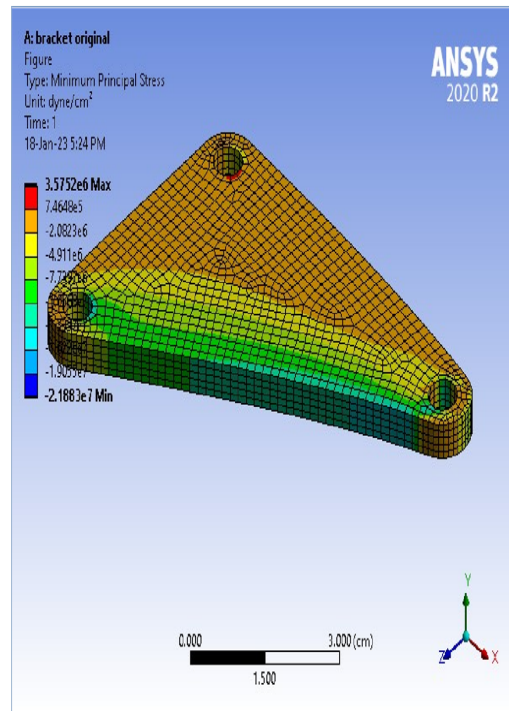


Figure 4.6: Minimum Principal Stress in original Bracket

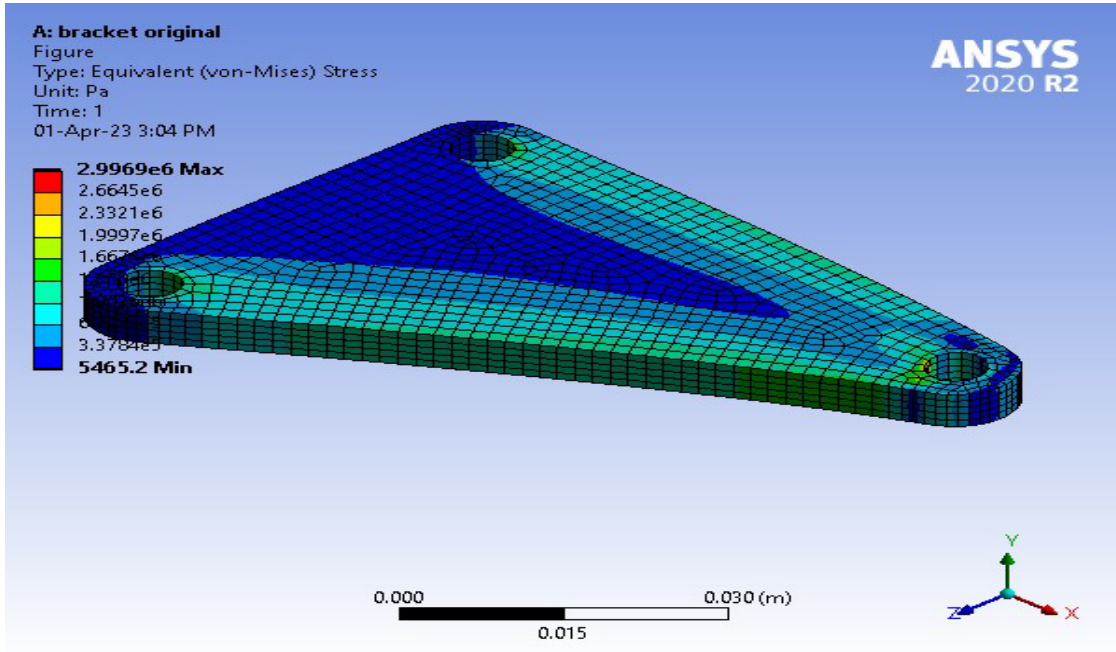


Figure 4.7: Equivalent Stress in original Bracket

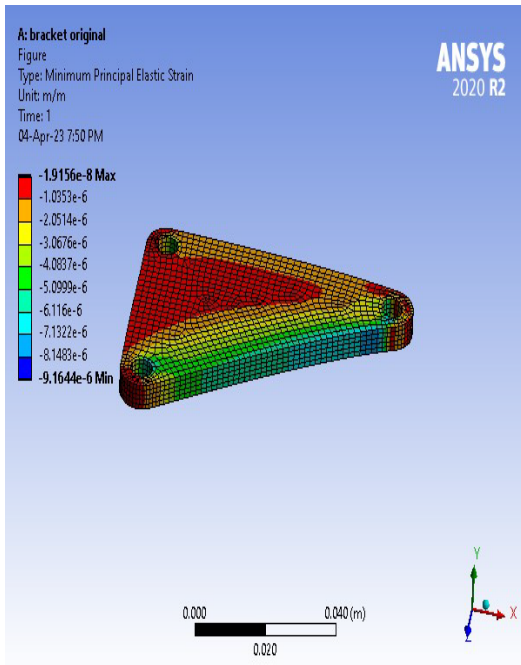


Figure 4.8: Maximum Principal Strain in original Bracket

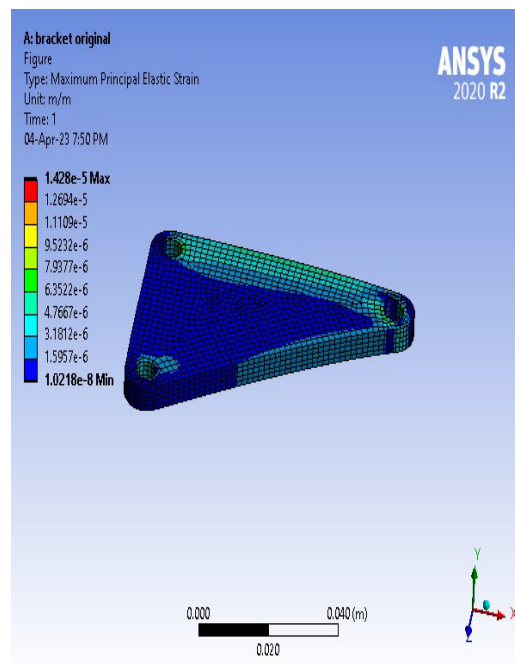


Figure 4.9: Minimum Principal Strain in original Bracket

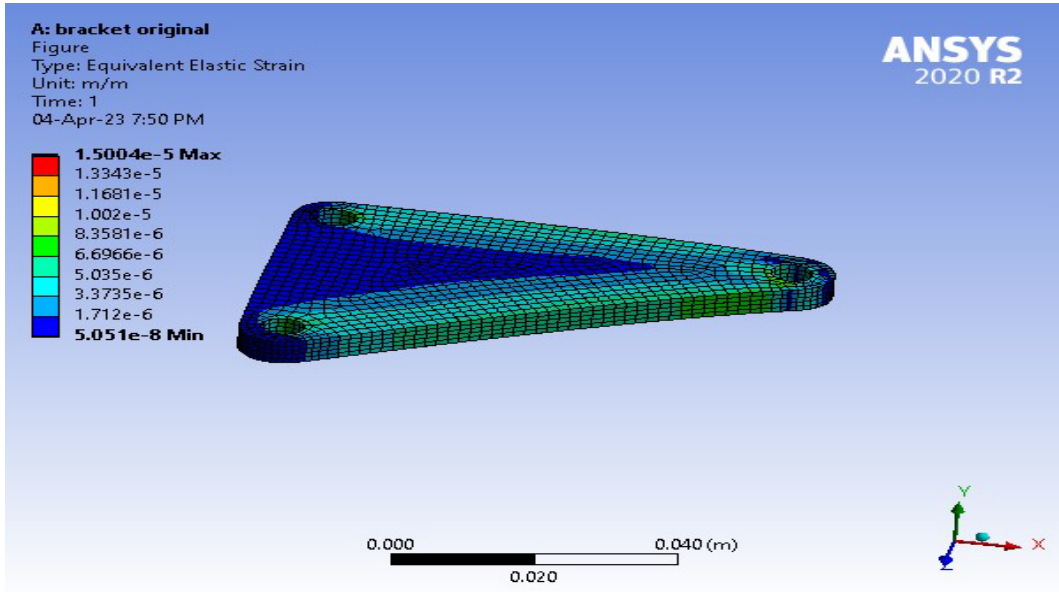


Figure 4.10: Equivalent Strain in original Bracket

4.3 Topology Optimization Analysis

We can eliminate the material of the Persian blue color portion from the bracket since it is not subjected to any stress. Drag Topology Optimization to the first analysis's "Results" cell. This will connect the topology optimization analysis and the static structural analysis shown in Figure 4.11.

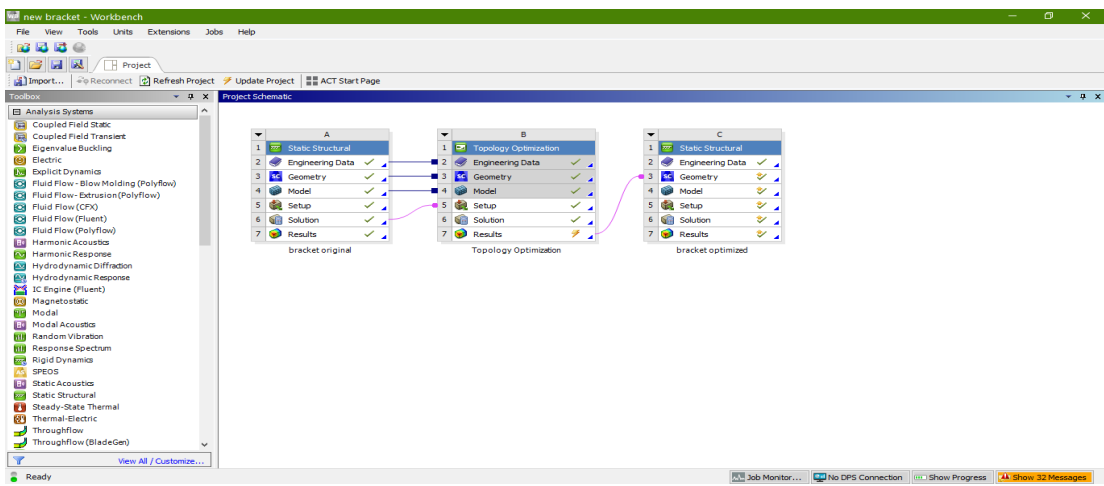


Figure 4.11: Topology Optimization on Workbench

Retain 65% of the mass by altering the response constraint. Make the system work. Figures 4.12 and 4.13 demonstrate this. Additionally, the Iteration table is in Table 4.4.

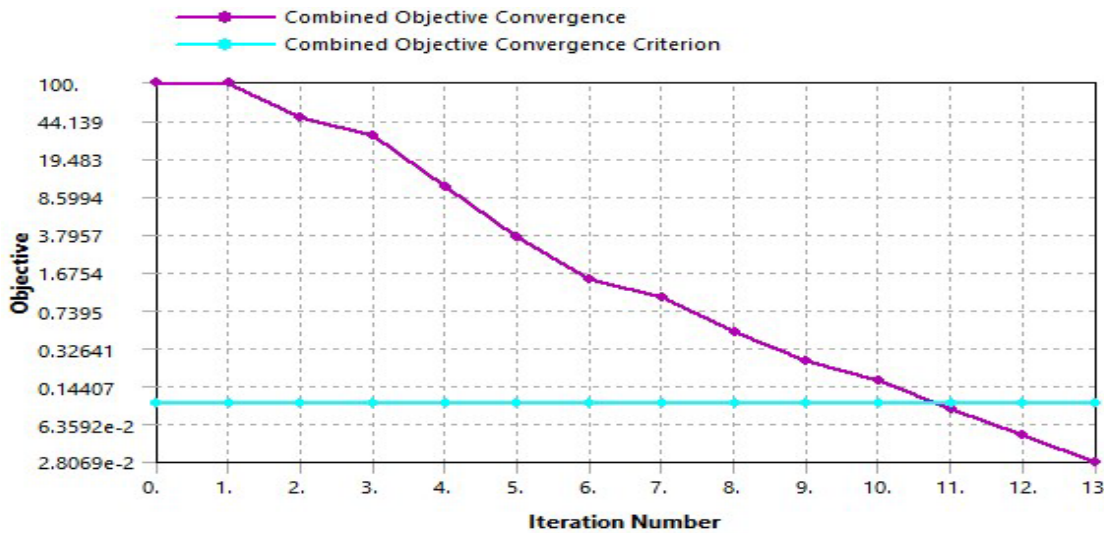


Figure 4.12: Graph between Objective and Iteration Number

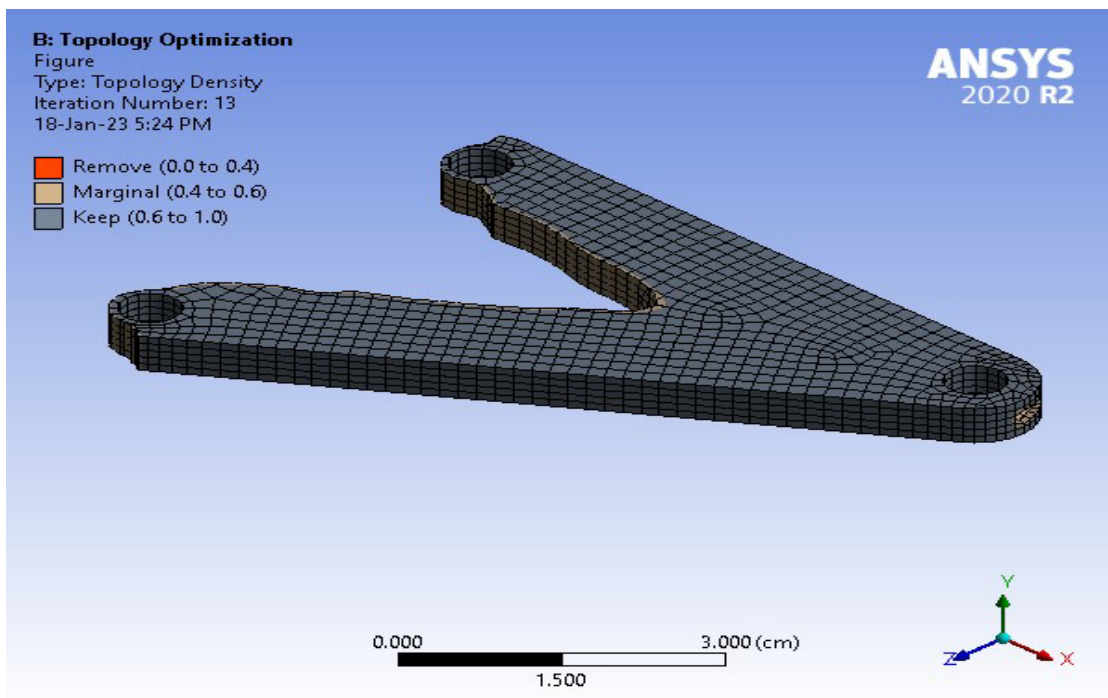


Figure 4.13: Topology Optimization of the Bracket

Table 4.4: Topology Optimization Iteration Table

Iteration	Minimum	Maximum	Average
1	0.65	1	0.669
2	0.40324	1	0.6602
3	0.1478	1	0.65204
4	1.e-003	1	0.65112
5	1.e-003	1	0.65365
6	1.e-003	1	0.65303
7	1.e-003	1	0.6523
8	1.e-003	1	0.65238
9	1.e-003	1	0.65243
10	1.e-003	1	0.65345
11	1.e-003	1	0.65524
12	1.e-003	1	0.65347
13	1.e-003	1	0.65364

4.4 Design Procedure of an Optimized Bracket

4.4.1 Modal Analysis

The STL file generated can be automatically exported into a new static structural analysis by performing a right-click on the cell Results on the topology optimization analysis and selecting "Transfer to Design Validation System." See the results of the STL import by opening SpaceClaim in the new analysis. The edges of the STL file should be copied to a new sketch plane.

Use the Fit Curves option under the Repair tab to streamline the rough curve geometry from the import. Choose Proper Tangency and stick with the 0.1mm preset distance. With the Trim Away tool and Make Corner tool, simplify the remaining geometry as necessary

shown in Figure 4.14.

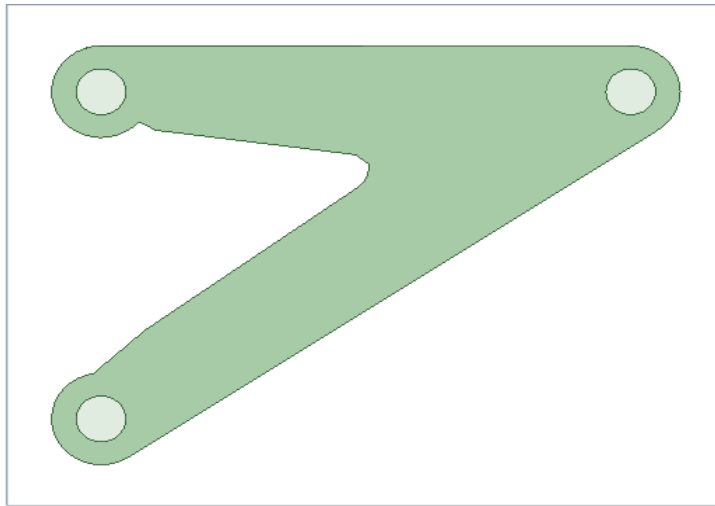


Figure 4.14: Topology Optimized Bracket

We utilize the repair tab's Merge Faces tool to combine selected faces into a single face in order to reduce the number of faces needed for mesh production. We must right-click on the products in the structure tree and select "Suppress for Physics" in order to exclude these items from the analysis and not export all product structure files into it. Only keep the Solid file. Click twice on the Model cell to close SpaceClaim and launch Mechanical. When asked to read upstream data, respond with a yes.

Reapply boundary conditions and loads while updating the mesh shown in Figure 4.15.

Make the tangential component free and add two cylindrical supports. 30N of the additional bearing load was added in the Z direction shown in Figures 4.16 and 4.17. And the values are shown in Table 4.5.

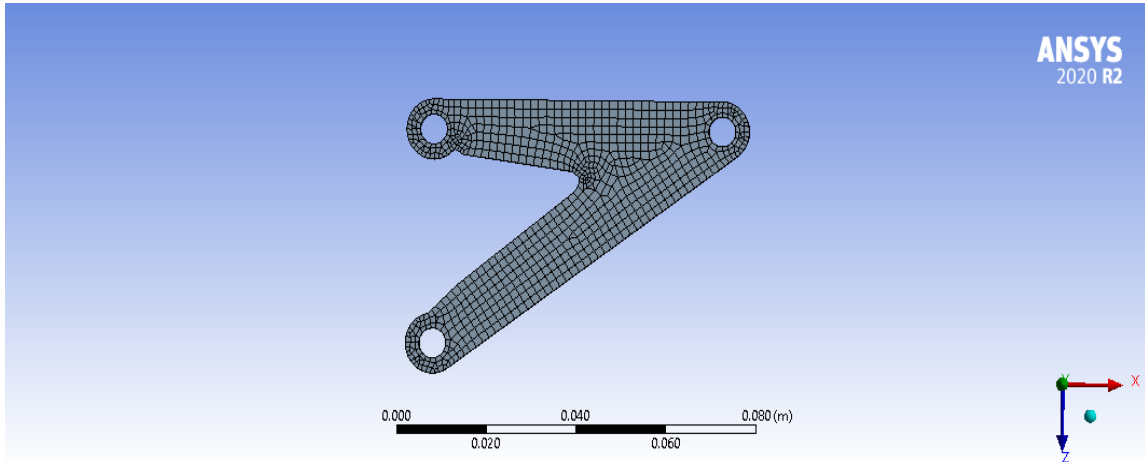


Figure 4.15: Triangular Bracket Mesh

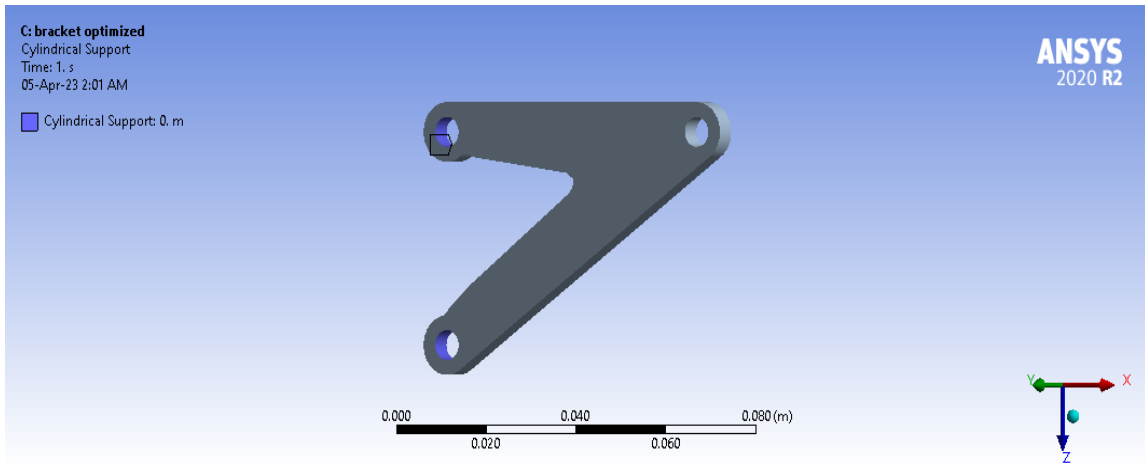


Figure 4.16: Optimized Bracket with cylindrical support

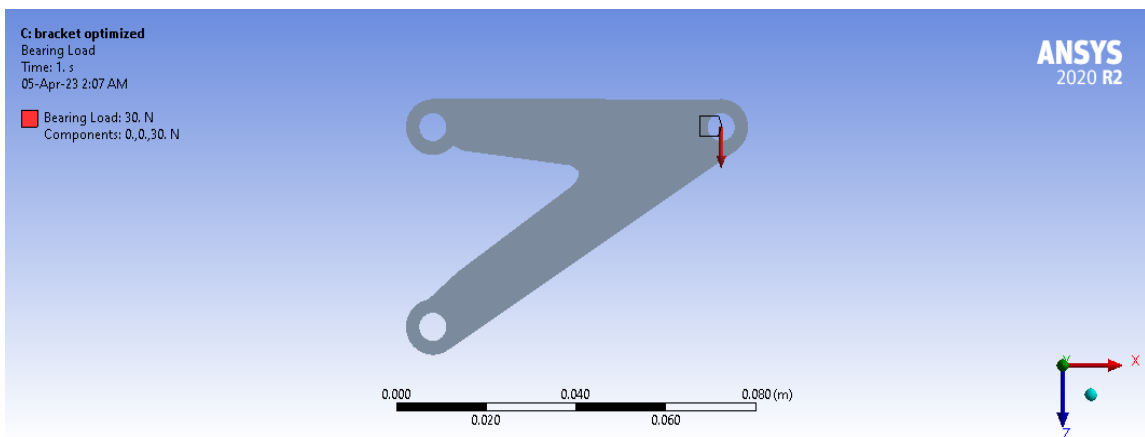


Figure 4.17: Optimized Bracket with Bearing Load

Solve to view the stress and strain results. In Table 4.6 and pictures 4.18, 4.19, and 4.20, the results of adding equivalent stress, as well as the maximum and minimum principal stress levels, are displayed. Also, the findings of the Equivalent Strain, Maximum Principal Strain, and Minimum Principal Strain of the bracket are provided in Table 4.7 and Figures 4.21, 4.22, and 4.23.

4.5 Optimized Bracket Analysis Report

Material	polycarbonate
Length X	7.6184 cm
Length Y	0.5 cm
Length Z	5.479 cm
Volume	8.777 cm ³
Mass	68.9 g
Nodes	27671
Elements	5663
Centroid X	-5.4478 cm
Centroid Y	0.75 cm
Centroid Z	1.8668 cm
Moment of Inertia Ip1	100.99 g·cm ²
Moment of Inertia Ip2	386.87 g·cm ²
Moment of Inertia Ip3	288.75 g·cm ²
Curvature Min Size	Default (4.6987e-003 cm)
Curvature Normal Angle	Default (70.395°)

Proximity Min Size	Default(4.6987e-003 cm)
Diagonal	9.3973 cm
Average Surface Area	3.2283 cm ²

Table 4.5: Load on the Optimized Bracket

Object Name	Bearing Load	Cylindrical Support
Geometry	1 Face	2 Face
X Component	0 N	
Y Component	0 N	
Z Component	30 N	
Suppressed	No	No
Radial		Fixed
Axial		Fixed
Tangential		Free

Table 4.6: Stresses in the Optimized Bracket

Object Name	Equivalent Stress	Minimum Principal Stress	Maximum Principal Stress
Minimum	12542 Pa	-4.6316e+005 Pa	-2.1929e+006 Pa
Maximum	2.8882e+006 Pa	2.7011e+006 Pa	3.4809e+005 Pa
Average	6.389e+005 Pa	2.8699e+005 Pa	-3.724e+005 Pa

Table 4.7: Strain in the Optimized bracket

Object Name	Equivalent Strain	Minimum Principal Strain	Principal Strain	Maximum Principal Strain
Minimum	6.282e-08	-9.126e-06		2.948e-06
Maximum	1.446e-05	-3.8717e-08		1.3821e-05
Average	2.128e-06	-2.292e-06		1.994e-06

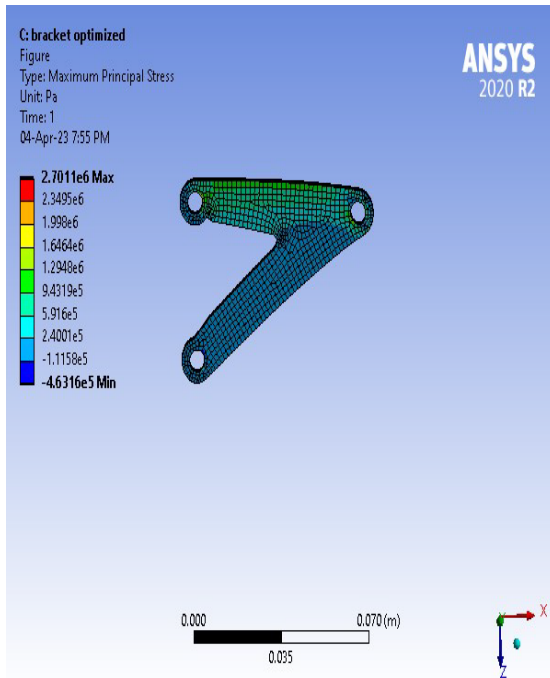


Figure 4.18 Maximum Principal Stress in Optimized Bracket

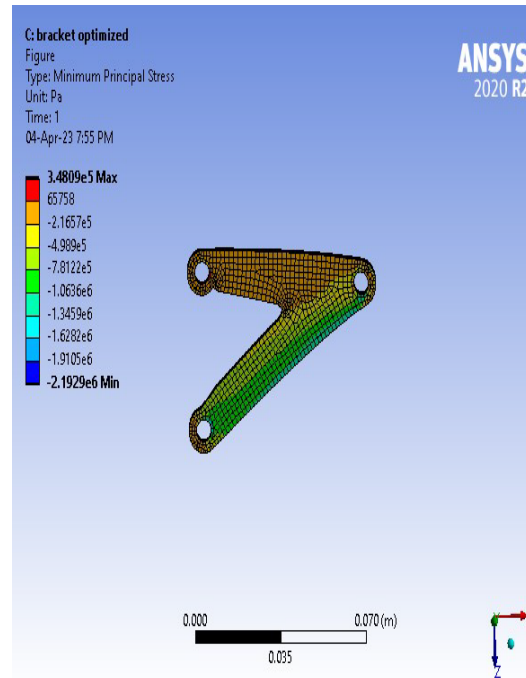


Figure 4.19: Minimum Principal Stress in Optimized Bracket

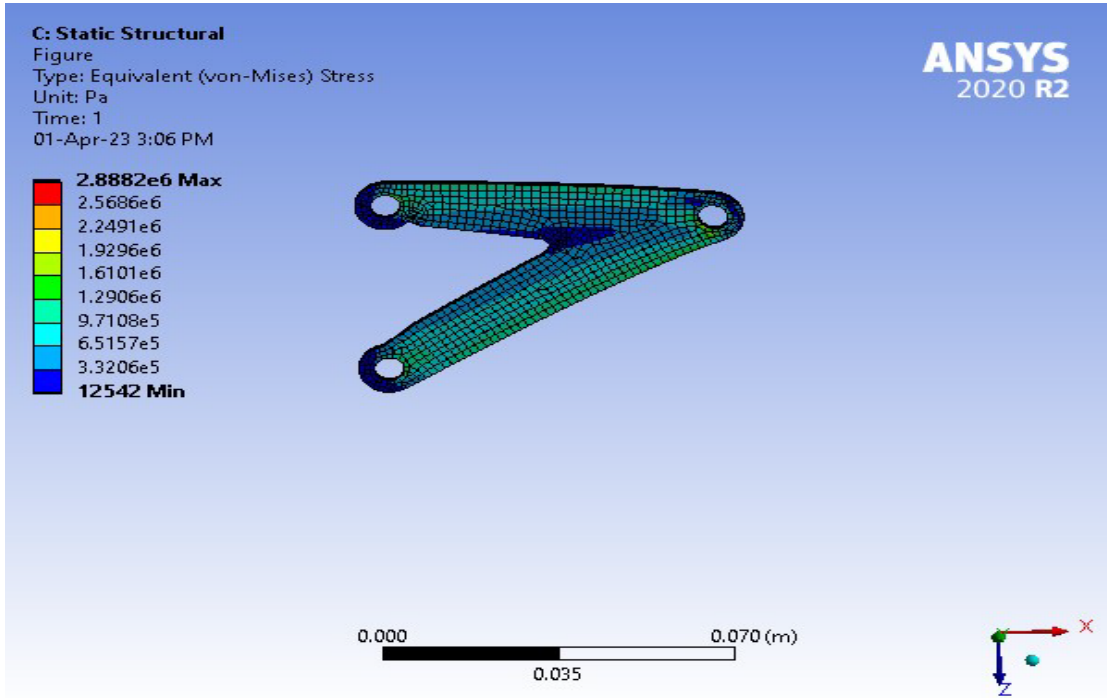


Figure 4.20: Equivalent Stress in Optimized Bracket

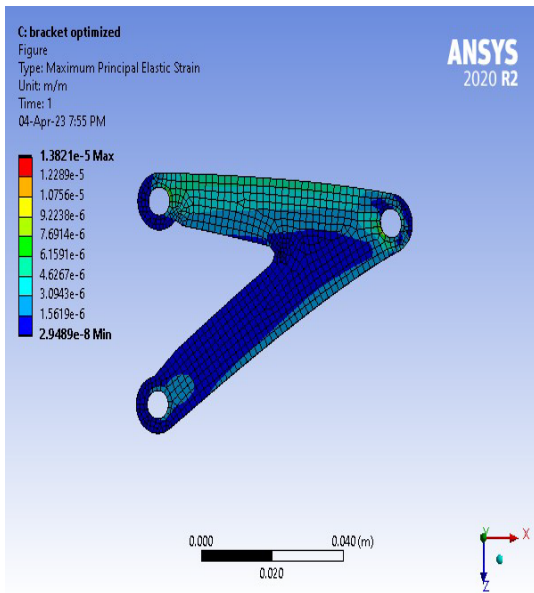


Figure 4.21: Maximum Principal Strain in Optimized Bracket

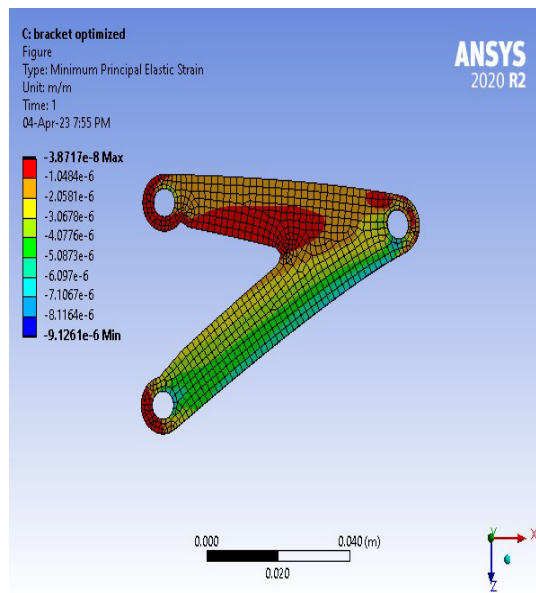


Figure 4.22: Minimum Principal Strain in Optimized Bracket

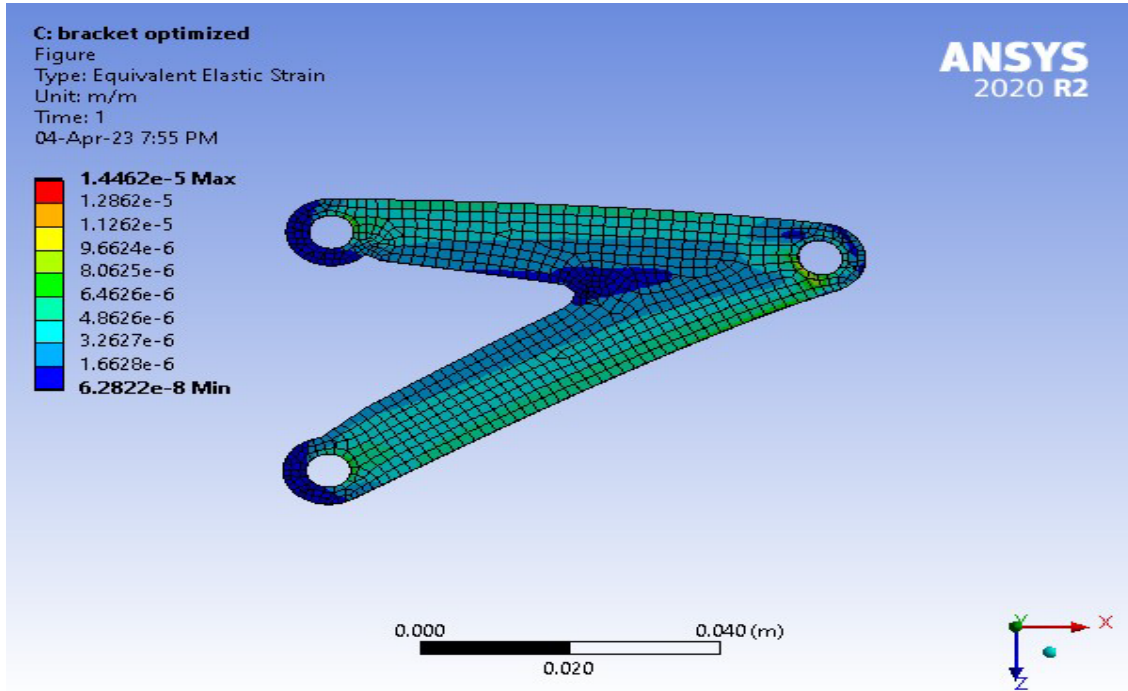


Figure 4.23: Equivalent Strain in Optimized Bracket

CHAPTER-5

PHOTOELASTIC EXPERIMENT AND ITS PROCEDURE

In this chapter we will discuss the Optical Polariscopes and its procedure. And deflection of the Triangular Bracket and the Optimized Bracket.

5.1 Description of Optical Polariscopes

A precise optical tool for measuring quantitative stress is called a polariscopes. The fundamental concept includes a mechanical drive coupling system for controlling all four filters, a polarizing assembly, an analyzing assembly, and other components. On a single base frame, all components are fixed. On ball bearings, the polarizer, analyzer, and rotate. A dial with fine engraving shows the direction of rotation. In use, the polariscopes is filled with a photoelastic model, and when forces are applied, a vibrant fringe pattern emerges. This pattern offers a clear image of the stress distribution throughout the entire model area. The capacity to perform the following types of analysis and measurement is provided by Polariscopes. The Optical Polariscopes figure is shown in Figure 5.1.

1. Overall assessment of nominal stress magnitude and gradients.
2. The directions of the principal stress.
3. The strength of the tangential stress sign along free (unloading) boundaries and in areas where stress is in a uniaxial state.
4. The size of the primary stress difference in a biaxial stress condition.

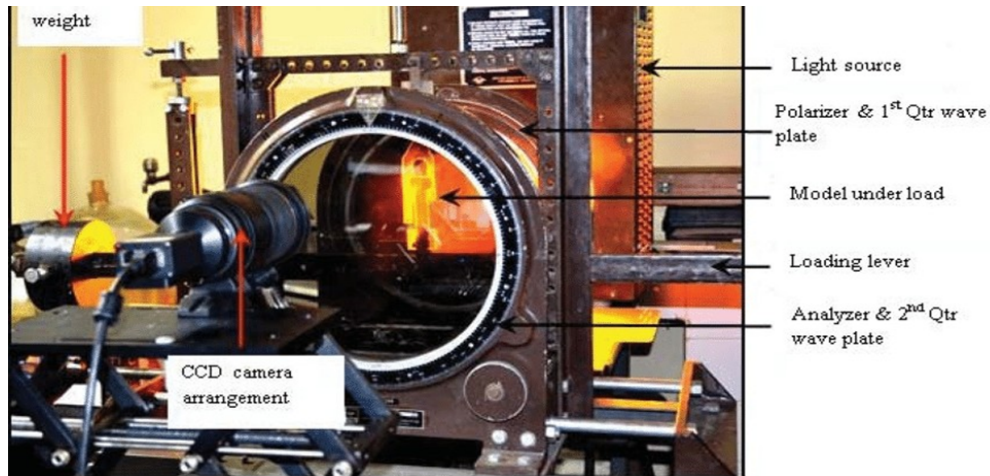


Figure 5.1: Optical Polariscopes

5.2 Experimental Procedure

Experimental Procedure setup is shown in 5.2.

1. Switch ON the monochromatic light source and allow it to attain full intensity.
2. Align the axis of the 'polarizer', 'Analyzer,' and 'Quarter wave plates' to obtain either a dark or bright field.
3. Fix the triangular bracket in the loading frame and bring the horizontal arm in position by means of balancing weights.
4. Load the triangular suitably and increase the load in equal steps and note the corresponding fringe order.
5. We built a stand and set a dial gauge on it. The dial gauge stand is fitted with triangular and Optimised brackets.
6. Place two polarized sheets in front of and behind the dial gauge stand. And put a white background at the rear. It serves as a source.
7. We will notice colors when we look at brackets from a polarized sheet.

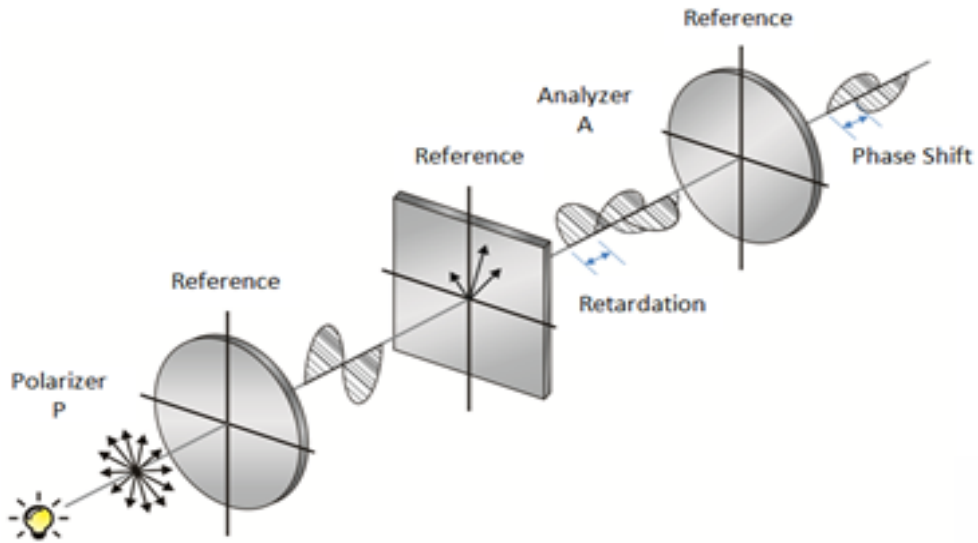


Figure 5.2: Photoelasticity Experiment

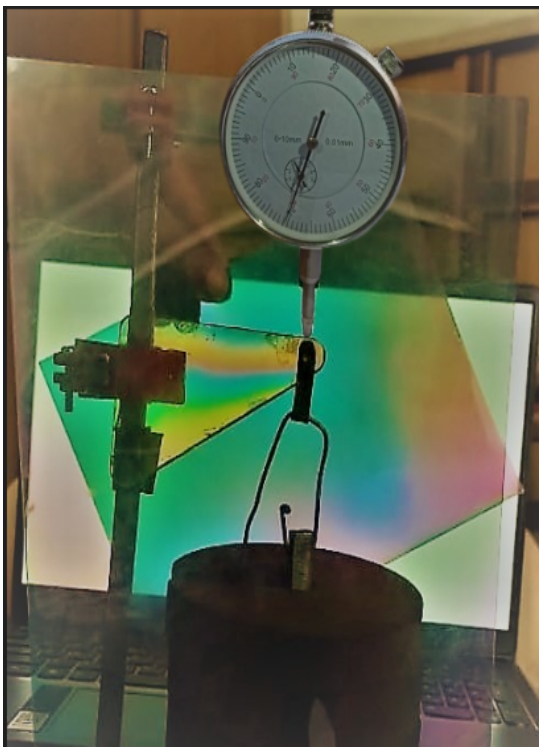


Figure 5.3: Dial gauge setup with Triangular Bracket

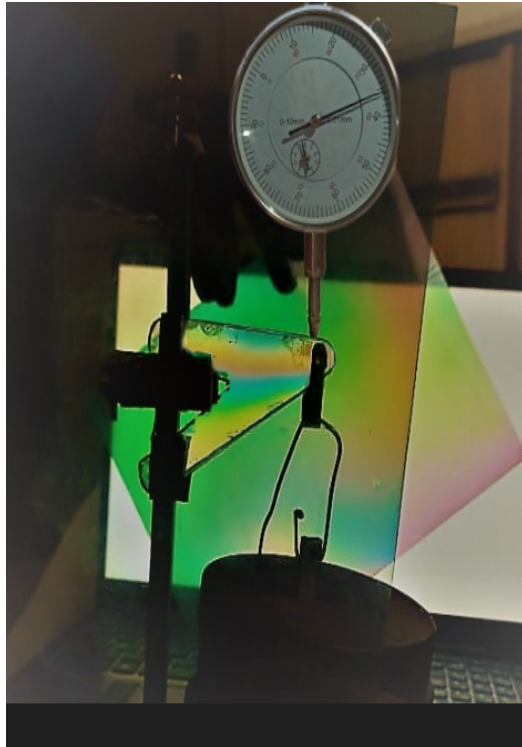


Figure 5.4: Dial gauge setup with Optimized Bracket

The bracket where the material is not required has been removed and optimized in the areas where the material is not required. After optimizing the bracket, approximately 65% of its mass is still retained.

When external pressure is placed on the bracket, both the original and optimized brackets display identical colors.

The amount of deflection observed in both the original and optimized brackets is almost identical.

5.3 Deflection in Dial Gauge

To determine the deflection of the triangular bracket and the optimized bracket, we set up a dial gauge stand.

For the dial gauge stand, we need four clamps. By 3d printing, we fabricate clamps for dial gauge setup. Clamps made via 3D printing are displayed in Figures 5.5 and 5.6.

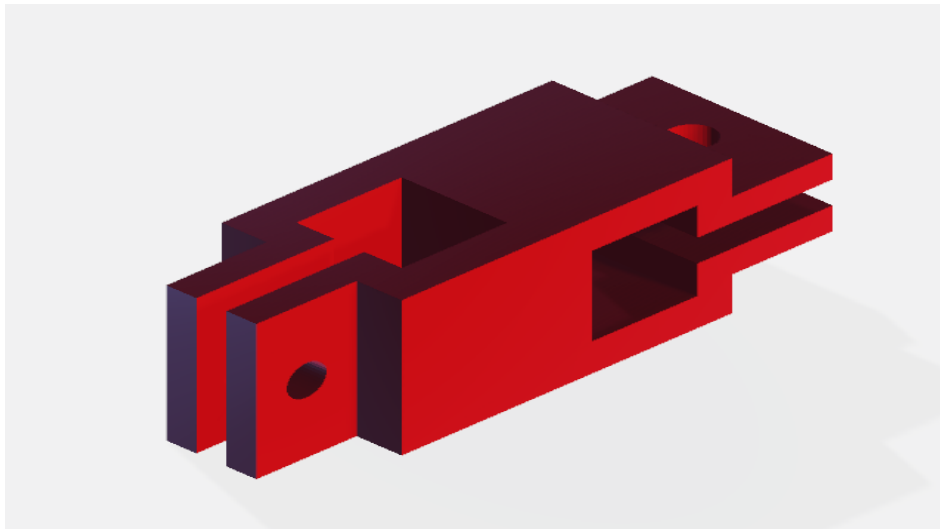


Figure 5.5: 3D Printing Clamp

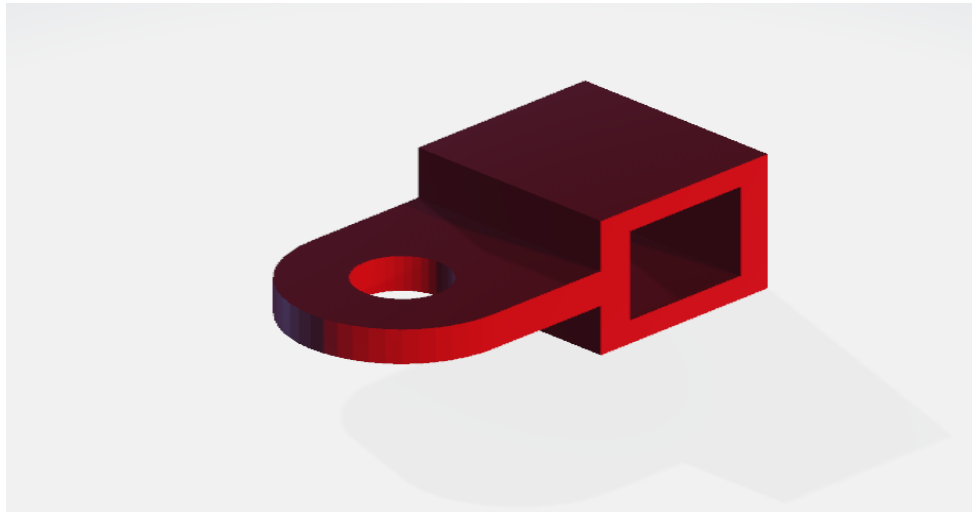


Figure 5.6: 3D Printing Clamp

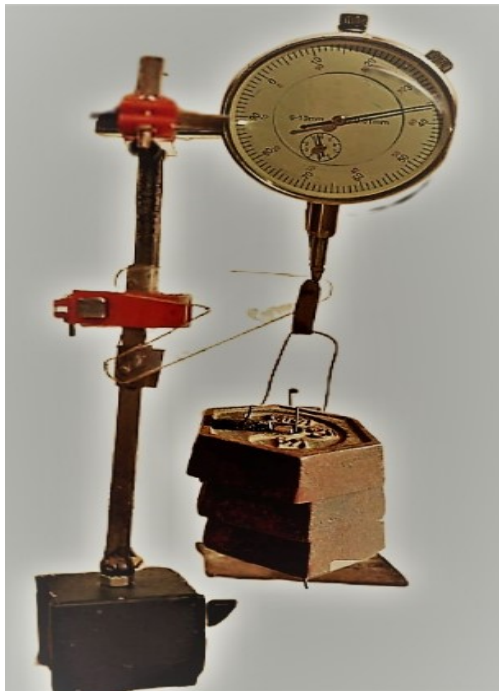


Figure 5.5: Dial Gauge setup for Optimized Bracket

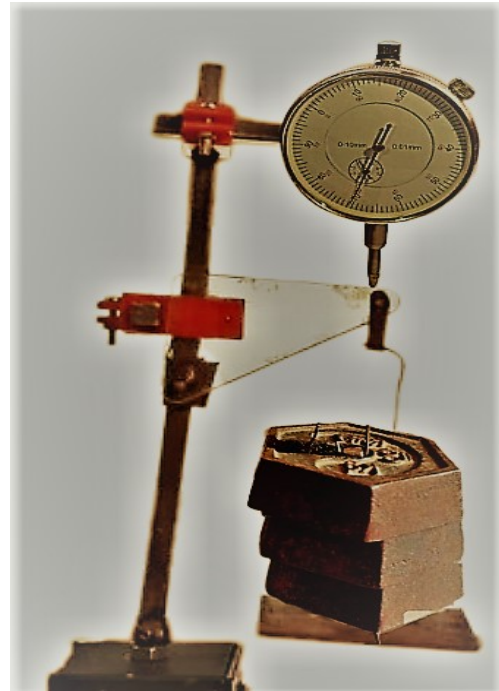


Figure 5.6: Dial Gauge setup for Triangular Bracket

Tables 5.1 and 5.2 show deflection values in both ranges for a 3 kg weight.

Dial Gauge Least Count = 0.01mm

Table 5.1: Dial Gauge Deflection Value in Triangular Bracket

Main Scale Reading (mm)	VSR (mm)	TR = MSR + (VC*LC) mm
1	71	1.71

Table 5.2: Dial Gauge Deflection Value in Optimized Bracket

Main Scale Reading (mm)	VSR (mm)	TR = MSR + (VC*LC) mm
1	30	1.30

We originally set the dial gauge reading to 3 mm since the load application is downward and it is not possible to position the dial gauge below the specimen. As a result, when the load is applied, the dial gauge plunger travels lower, and the reading is recorded in reverse order and deducted from the original value. The same process is used for the optimized bracket.

Initial Deflection Value = 3.00mm

When we apply a 3 kg force to a Triangular Bracket, the Dial Gauge Deflection = 1.71mm

When we apply a 3 kg force to a Optimized Bracket, the Dial Gauge Deflection = 1.30mm

Deflection in Bracket = Initial Deflection Value – Dial Gauge Deflection

Deflection in Triangular Bracket = 3.00 - 1.71 = 1.29mm

Deflection in Optimized Bracket = 3.00 - 1.30 = 1.70mm

There is a minor deflection variation between the Triangular and Optimized Brackets.

CHAPTER-6

RESULTS AND COMPARISON

Stresses and Strain results of the Triangular Bracket performed in Ansys. Tables 6.1 and 6.2 reveal the maximum, minimum, equivalent stress, and strain data, while figures 6.1, 6.2, and 6.3 illustrate the stresses. Figures 6.4, 6.5, and 6.6 depict strains.

Table 6.1: Stresses in the Triangular bracket

Object Name	Equivalent Stress	Minimum Principal Stress	Maximum Principal Stress
Minimum	5465.2 Pa	-2.1883e+006 Pa	4.5562e+005 Pa
Maximum	2.9969e+006 Pa	3.5752e+005 Pa	2.7801e+006 Pa
Average	5.2335e+005 Pa	-3.1166e+005 Pa	2.3117e+005 Pa

Table 6.2: Strain in the Triangular bracket

Object Name	Equivalent Strain	Minimum Principal Strain	Maximum Principal Strain
Minimum	5.051e-08	-9.1644e-06	1.0218e-08
Maximum	1.5e-05	-1.915e-08	1.28e-05
Average	2.638e-06	-1.906e-06	1.622e-06

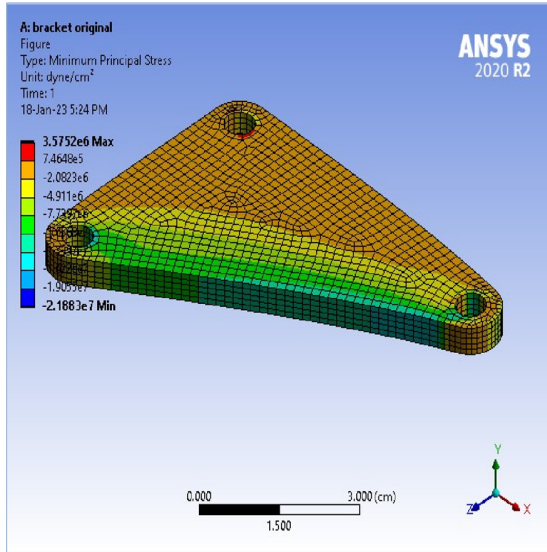


Figure 6.1: Minimum Principal Stress (original Bracket)

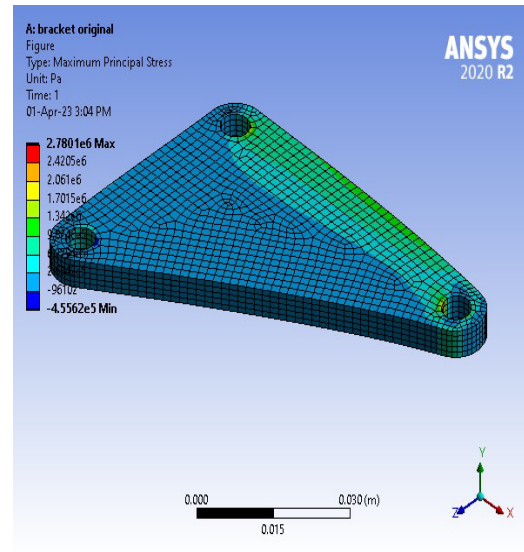


Figure 6.2: Maximum Principal Stress (original Bracket)

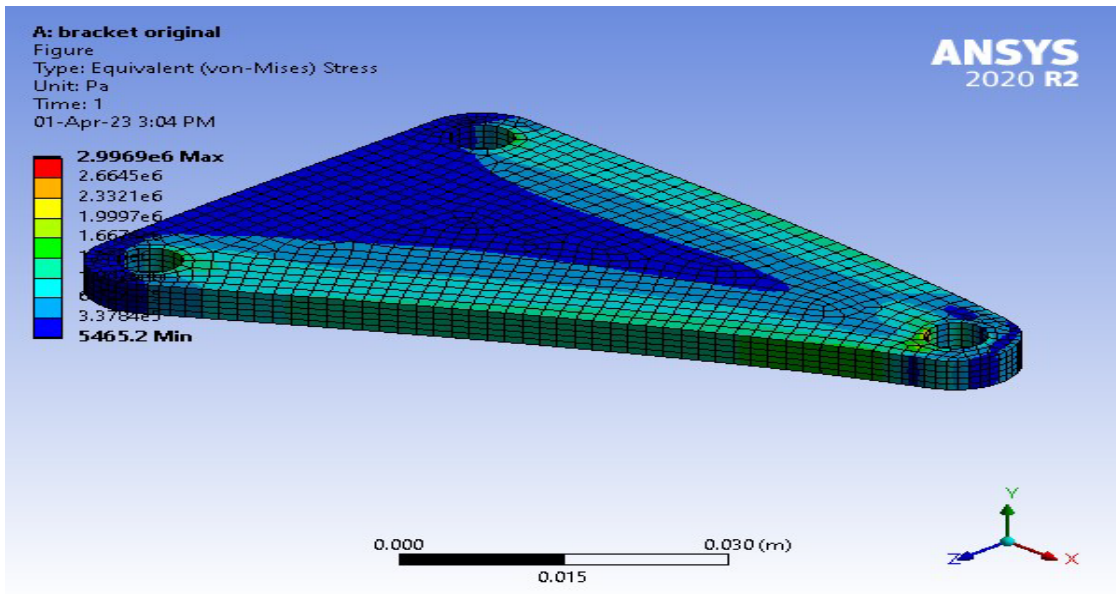


Figure 6.3: Equivalent Stress (original Bracket)

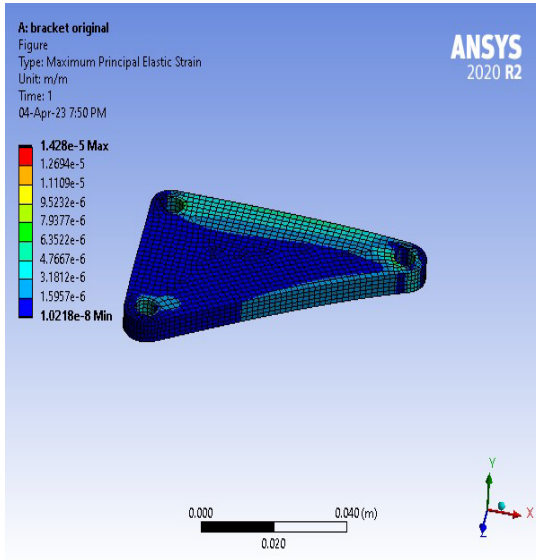


Figure 6.4: Maximum Principal Strain (original Bracket)

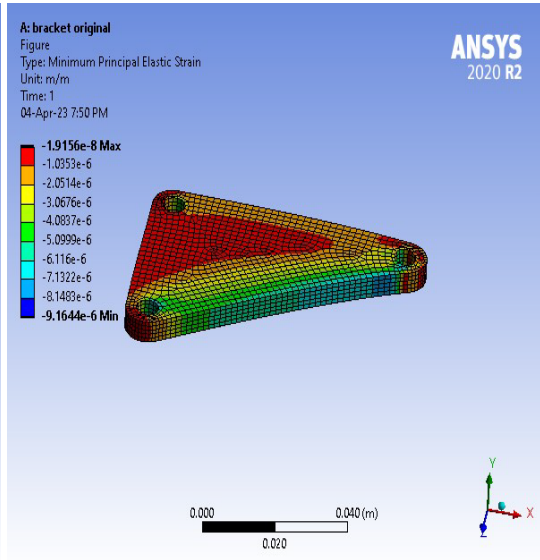


Figure 6.5: Minimum Principal Strain (original Bracket)

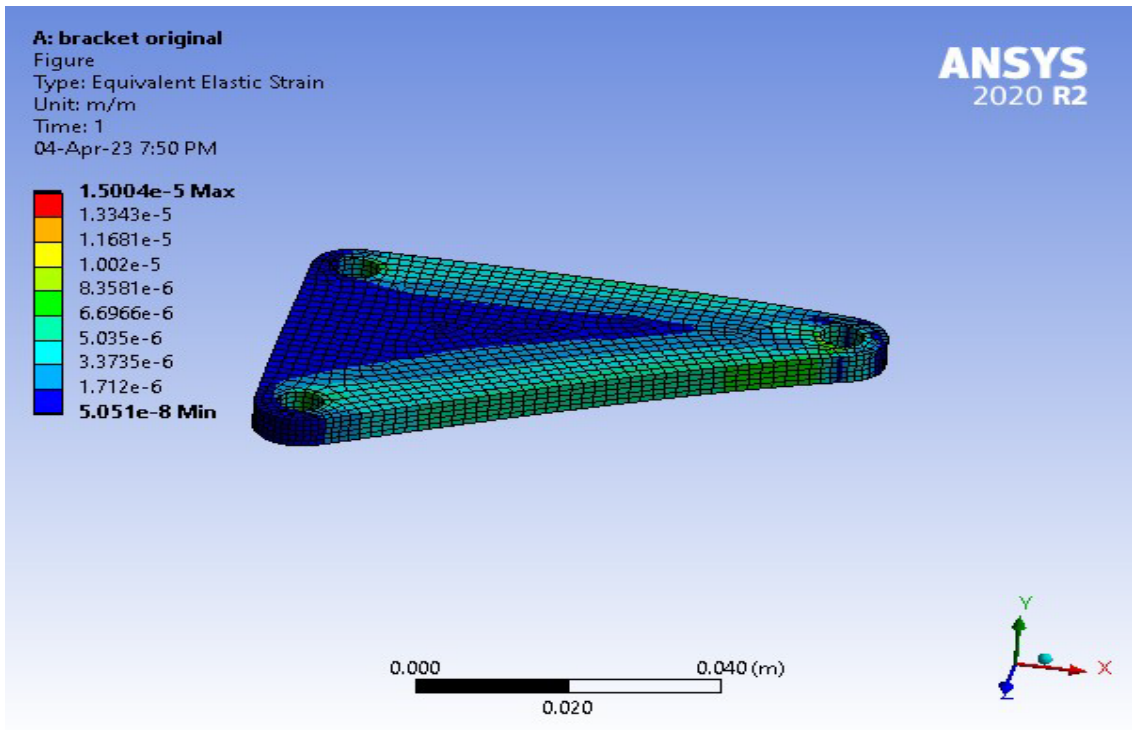


Figure 6.6: Equivalent Strain (original Bracket)

Stresses and Strain results of the Optimized Bracket performed in Ansys. Tables 6.3 and 6.4 reveal the maximum, minimum, equivalent stress, and strain data, while figures 6.7, 6.8, and 6.9 illustrate the stresses. Figures 6.10, 6.11, and 6.12 depict strains.

Table 6.3: Stresses in the Optimized Bracket

Object Name	Equivalent Stress	Minimum Principal Stress	Maximum Principal Stress
Minimum	12542 Pa	-4.6316e+005 Pa	-2.1929e+006 Pa
Maximum	2.8882e+006 Pa	2.7011e+006 Pa	3.4809e+005 Pa
Average	6.389e+005 Pa	2.8699e+005 Pa	-3.724e+005 Pa

Table 6.4: Strain in the Optimized bracket

Object Name	Equivalent Strain	Minimum Principal Strain	Maximum Principal Strain
Minimum	6.282e-08	-9.126e-06	2.948e-06
Maximum	1.446e-05	-3.8717e-08	1.3821e-05
Average	2.128e-06	-2.292e-06	1.994e-06

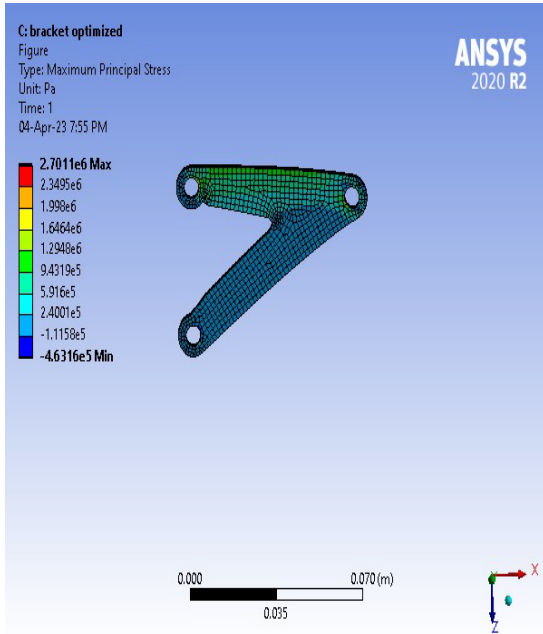


Figure 6.7: Maximum Principal Stress (Triangular Bracket)

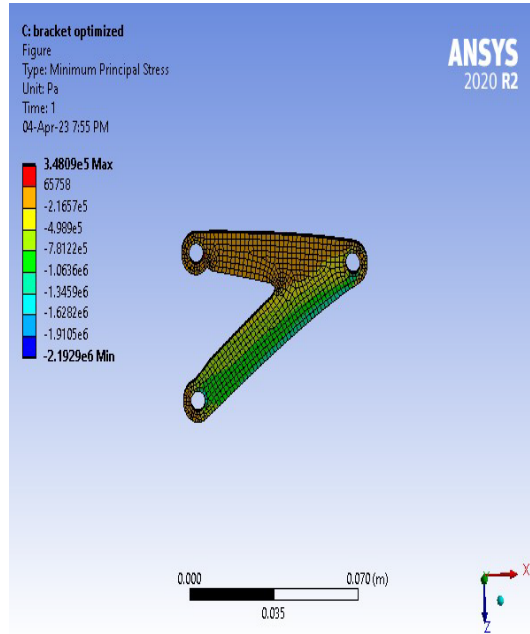


Figure 6.8: Minimum Principal Stress (Triangular Bracket)

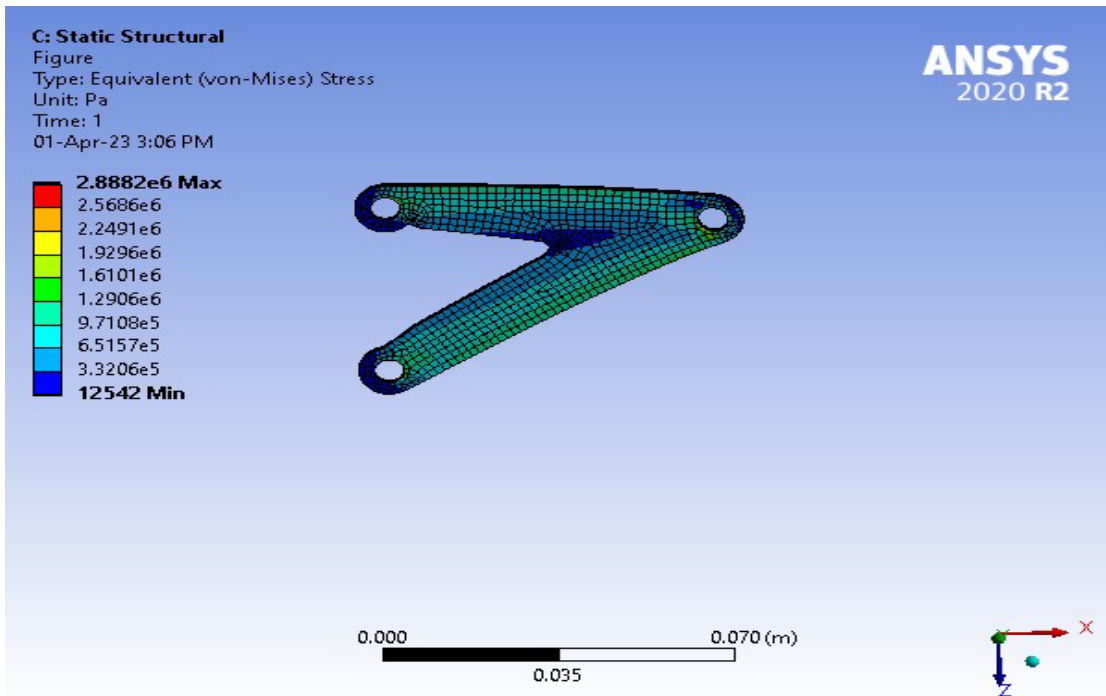


Figure 6.9: Equivalent Stress (Optimized Bracket)

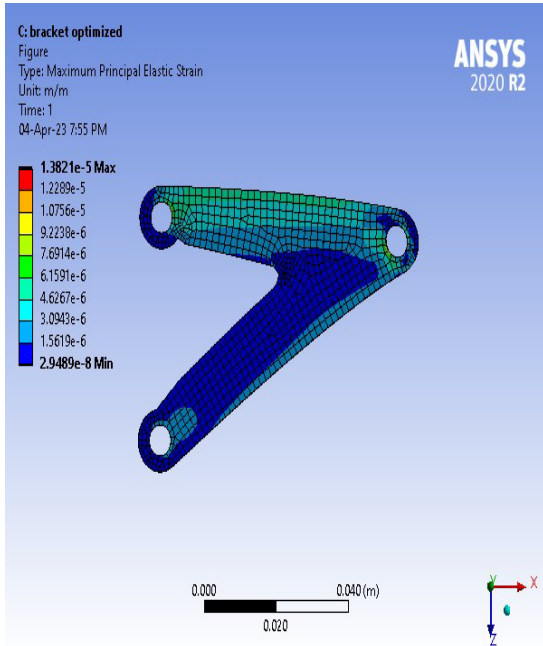


Figure 6.10: Maximum Principal Strain (Optimized Bracket)

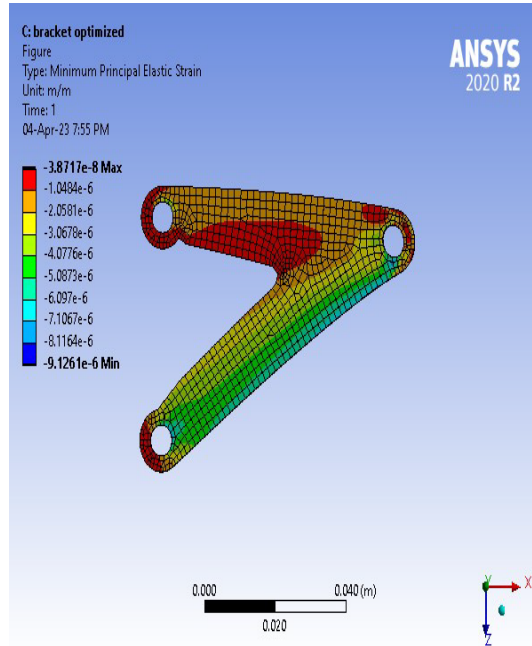


Figure 6.11: Minimum Principal Strain (Optimized Bracket)

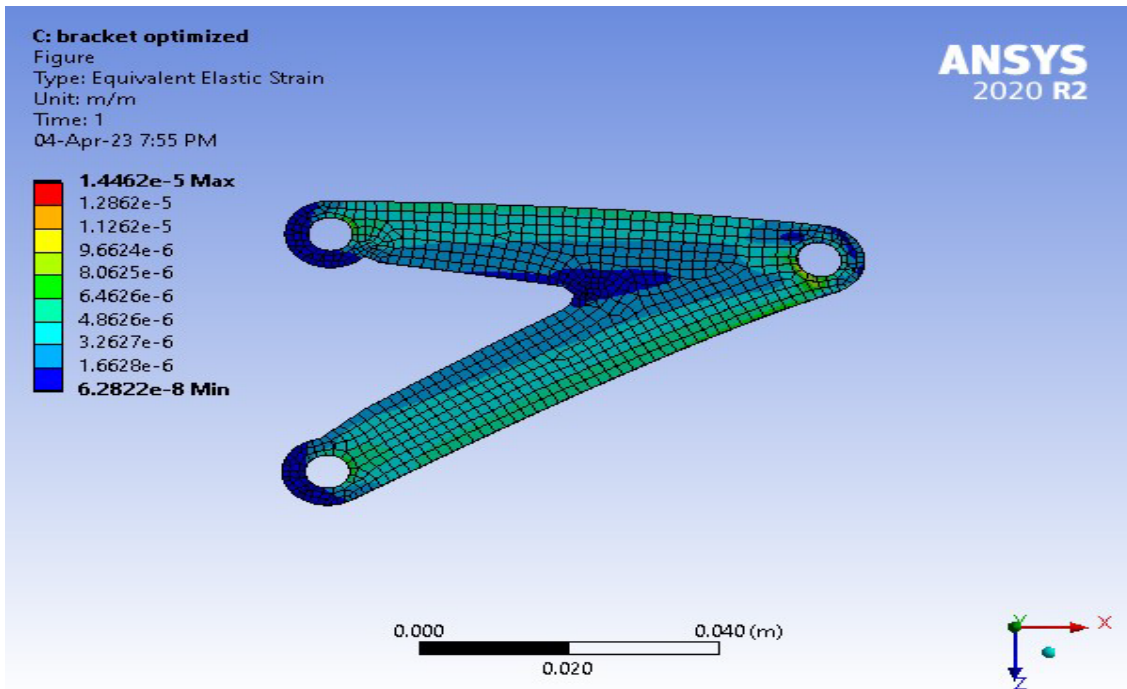


Figure 6.12: Equivalent Strain (Optimized Bracket)

Since this is the result of a stress and Strain analysis in Ansys. As a result of this triangular bracket, the Minimum Principal Stress is -4.6316×10^5 Pa (minimum stress), 2.7011×10^6 Pa (maximum stress), and the Maximum Principal Stress is -2.1929×10^6 Pa (minimum stress), and 3.4809×10^5 Pa (maximum stress). The Triangular Bracket is Minimum Principal Strain is -9.126×10^{-6} (minimum strain), -3.8717×10^{-8} (maximum strain), and the Maximum Principal Strain are -2.948×10^{-6} (minimum strain), and 1.3821×10^{-5} (maximum strain).

As a result of this Optimized Bracket, the Minimum Principal Strain is -4.6316×10^5 Pa (minimum strain), 2.7011×10^6 Pa (maximum strain), and the Maximum Principal Stress are -2.1929×10^6 Pa (minimum strain), 3.4809×10^5 Pa (maximum strain). The Optimized Bracket's Minimum Principal Strain is -9.126×10^{-6} (minimum strain), -9.126×10^{-6} (maximum strain), and the Maximum Principal Strain is 2.948×10^{-6} (minimum strain), and 1.3821×10^{-5} (maximum strain).

The deflection indicated by the dial gauge in both brackets is almost equal.

If you compare the two results, the stresses, and the deformation in both brackets are almost the same. So we can remove the extra material from the bracket. We can reduce the size of the Bracket. By optimizing the design of a product, we can identify weak spots and areas prone to wear and tear. It often prevents the waste of unfinished materials and other resources.

CHAPTER-7

CONCLUSION

7.1 Conclusions

In this project, we examined the topology optimization of a bracket in ANSYS under a 30N load. As a result of our analysis, we found the equivalent stress, maximum principal stress, minimum principal stress, and Strain of the original bracket, and the optimized bracket.

- To determine bracket deflection, we assembled a dial gauge. By comparing both experimental and analytical stress values, we observed that the stresses and Strain of both the original and triangular brackets are nearly identical.
- As a result, we can save a considerable amount of material. Make the bracket smaller and lighter in weight.
- By optimizing the design of a product, we can identify weak spots and areas prone to wear and tear.

7.2 Future Scope of Work

A crucial component of cutting-edge medical technology, particularly in implants and prosthetics, is topology optimization. To design effective prosthetic parts, our algorithm mimics the bone density and stiffness of the human body.

A crucial component of cutting-edge medical technology, particularly in implants and prosthetics, is topology optimization. To design effective prosthetic parts, our algorithm mimics the bone density and stiffness of the human body.

Most of the existing techniques in the manufacturing sector can be improved upon or improved still more, for example by concurrently optimizing the build direction while doing overhang-free topology optimization. Moreover, several techniques, including the resilient topology optimization approaches and the heterogeneous two-scale topology optimization algorithm, have not been directly connected to or confirmed by AM.

REFERENCES

- [1] Hirmukhe, S. S., & Dhatrak, P. N.,” Photoelastic Stress Analysis”, A Review. IOSR Journal of Mechanical & Civil Engineering.
- [2] Pathak, P. M., and K. Ramesh. “Analysis for Photoelasticity using Image Processing Technique”, International Journal of Software Engineering & its Applications.
- [3] Felippa, Carlos A. "On the use to build photoelastic models for stress analysis investigations." Materials & design.
- [4] Haciane, Rabah “Experimental Stress Analysis of Composite Circular Disc”, IOSR Journal of Mechanical & Civil Engineering.
- [5] Etsion, Maxwell, J. C Biomechanics studies in dentistry: “Bioengineering applied oral implantology”, International Journal for Numerical Methods in Biomedical Engineering.
- [6] Hughes, Mark, Digital photoelasticity: Recent developments and diverse applications. Society for Experimental Stress Analysis.
- [7] Loqman, A., Stunadar, A., Kan, J. C. H., Ze, C. G., & Kang, C. S “ A simple evolutionary procedure for structural optimization”, University of Sydney.
- [8] T. H Baek., Kim, M. S., & Hong, D. P. Fringe “ Application of topology, sizing, and shape optimization method”, University of Colorado Boulder.
- [9] Bhimaraju, H. S. Narasimha,” Support structure-constrained topology optimization for additive manufacturing”, School of Mechanical & Production Engineering Technological University.
- [10] Patil, Rupali, and Er NK Patil,” Evolutionary Topology Optimization of Continuum Structures - Methods and Applications”.

- [11] Frankovský. P., and F. Trebuňa,” Topology optimization of non-linear elastic structures and compliant mechanisms”.
- [12] Karalekas, D. E., and A. Agelopoulos” Length scale and manufacturability in density-based topology optimization”, University of Colorado Boulder.
- [13] Lalitha, T., & Purushotham, D. A,” Topology optimization of non-linear elastic structures and compliant mechanisms”, IOSR Journal of Mechanical & Civil Engineering.

